Supplementary Material for

Urine and serum metabolic profiling combines machine learning for autoimmune diseases discrimination and classification

Qiuyao Du[1,2], Xiao Wang[1,2], Junyu Chen[1,2], Caiqiao Xiong [1,2], Wenlan Liu[3], Jianfeng Liu[4], Huihui Liu[1,2]*, Lixia Jiang[4]* & Zongxiu Nie[1,2]*

[1]Beijing National Laboratory for Molecular Sciences, Key Laboratory of Analytical Chemistry for Living Biosystems, Institute of Chemistry, Chinese Academy of Sciences, Beijing 100190, China.
[2]University of Chinese Academy of Sciences, Beijing 100049, China.
[3] The Center for Medical Genetics & Molecular Diagnosis, Shenzhen Second People's Hospital/the First Affiliated Hospital of Shenzhen University Health Sciences Center, Shenzhen 518035, China.
[4]Department of Laboratory Medicine, First Affiliated Hospital of Gannan Medical University, Ganzhou, Jiangxi Province 341000, China.

Correspondence should be addressed to Huihui Liu; hhliu@iccas.ac.cn, Lixia Jiang; jlx7310@gmu.edu.cn and Zongxiu Nie; znie@iccas.ac.cn

This part included:

Materials and methods

Biological samples

This study complied with the ethical standards formulated by the Hospital Scientific Research Ethics Committee of First Affiliated Hospital of Gannan Medical University (the serial number of the approval is LLSC-2021071301), and obtained the subject's informed consent. Urine and serum samples were collected from 247 subjects included 127 healthy controls (HC) and 120 patients with autoimmune diseases (ADs) in 2 mL centrifuge tubes and stored in a fridge at -80 °C. After excluding 84 individuals (65 HC and 19 ADs), the remaining samples were used for discriminant analysis. The gender and age distribution of the study participants were listed in Table S1. A two-tailed student's t-test was applied for age comparisons between two groups, and the obtained p value was $0.484 > 0.05$. To assess differences across the gender, a chi-squared test was used and resulting in a p-value of $0.077 > 0.05$. The results indicated that there were no statistically significant differences in the age and gender of the subjects.

Chemicals

N-(1-naphthyl)ethylenediamine dihydrochloride (NEDC) was supplied by Sigma-Aldrich (St Louis, MO, USA). Uric acid, 2,5-dihydroxybenzoic acid (DHB) and 1-naphthylhydrazine hydrochloride (NHHC) were provided by J&K (Beijing, China). Graphdiyne (GD), cubic boron nitride (c-BN) and hexagonal boron nitride (h-BN) were purchased from Xianfeng Nanotechnology Corporation (Nanjing, China). Glucose was obtained from Sinopharm Chemical Reagent Co., Ltd (Shanghai, China). 3-chloro-L-phenylalanine was provided by Aladdin Biochemical Technology Co., Ltd (Shanghai, China). D-glucose-1,2-$^{13}C_2$ was purchased from Cambridge Isotope Laboratories Inc (USA). Methanol, ethanol, acetonitrile and trifluoroacetic acid (TFA) were obtained from Fisher Scientific (USA). The water used was prepared by a Milli-Q water purification system from Millipore (Milford, MA, USA).

Standard solutions

0.1 mg/mL and 0.05 mg/mL GD, 0.25 mg/mL c-BN and h-BN were prepared by dissolving them in deionized water. NHHC were prepared at the concentrations of 10 mg/mL in 50% methanol aqueous solution. 10 mg/mL NEDC was prepared by dissolving in 30% ethanol aqueous solution. DHB was prepared at the concentration of 10 mg/mL in 50% acetonitrile aqueous solution which containing 0.1% TFA. 3-chloro-L-phenylalanine was prepared at the concentration of 10 mmol/L in 50% methanol aqueous solution and used as the internal standard in urine samples. A series of uric acid standard solutions were prepared with concentration ratios of uric acid / 3-chloro-L-phenylalanine at 0.030, 0.038, 0.045, 0.075, 0.090 and 0.120. 5 mmol/L D-glucose-1,2-$^{13}C_2$ aqueous solution was used as the internal standard in serum samples and series glucose standard solutions with concentration ratios of glucose / D-glucose-1,2-$^{13}C_2$ at 0.16, 0.24, 0.40, 0.48, 0.80 and 2.00 were prepared. The solutions were stored at 4°C in darkness.

Sample preparation

For serum samples, acetonitrile was added at a ratio of 1:2 to a 10 μL serum sample

to precipitate proteins. The supernatant was collected for matrix-assisted laser desorption/ionization mass spectrometry (MALDI-MS) analysis. Urine samples are not subjected to any pretreatment. Equal volumes (1 μL) of the serum supernatant or urine sample, internal standard solution and matrix solution (NEDC) were mixed and 1 μL of the resulting solution was deposited on the MALDI target plate and air-dried for further MS analysis. Quality control (QC) samples were prepared by combining equal volumes of all the urine or serum samples separately and then prepared as described above for instrumental analysis. QC samples were analyzed every six samples of the sequence to stabilize instrument performance and adjust signal drift between samples. Three mass spectra were acquired from independent experiments for each sample. The overall performance of the mass spectrometer was checked in every experiment using an oligosaccharides standard (D-glucose (MW: 180.16), maltose (MW: 342.30), 1-kestose (MW: 504.4), nystose (MW: 666.6), 1,1,1-kestopentaose (MW: 828.7), fructo-oligosaccharide DP6 (MW: 990.86)) before each run.

MALDI-Time-of-flight (TOF) MS analysis

MALDI-TOF MS analysis was performed in reflection negative mode using a Bruker Ultraflextreme mass spectrometer (Bruker Daltonics, Billerica, Germany) equipped with a 355 nm smart beam Nd:YAG pulsed laser, within a mass range of 0-1000 Da. Each mass spectrum was obtained as an average of 200 laser shots at 500 Hz, and the laser size and laser power energy were set to ultra and 50% respectively.

MALDI-Fourier transform ion cyclotron resonance (FTICR) MS analysis

MALDI-FTICR MS analysis was performed with a Bruker 15 T SolariX FTICR mass spectrometer (Bruker Daltonics, Billerica, Germany) equipped with a 355 nm smart beam Nd:YAG pulsed laser. Metabolite identification was achieved by comparing high-resolution MS spectra with the online metabolomic databases: The Human Metabolome Database (HMDB, https://www.hmdb.ca/).

High performance liquid chromatography (HPLC) MS/MS analysis

HPLC-MS/MS analysis was performed on a 1260 HPLC instrument (Agilent Technologies, Palo Alto, CA, USA) and a Bruker Impact HD Q-TOF mass spectrometer (Bruker Daltonics, Billerica, Germany). A ZORBAX Eclipse Plus C18 column (100 × 4.6 mm, 3.5 μm) was used for the separation of analytes.

Statistical analysis

MALDI-MS data processing was performed using flexAnalysis 3.4 software with the signal to noise (S/N) of peaks over three. Peak normalized was performed on home-built code in Python 3.7. Specifically, urine and serum samples were collected from 247 subjects. After excluding 84 individuals (age and gender comparisons), 62 HC and 101 patients with ADs were included for subsequent analyses. The collected urine and serum samples were separately mixed with matrix and internal standard (IS) according to the above steps and subsequently entered the mass spectrometer for analysis. Each sample was tested 3 times in parallel. During the machine learning process, we randomly separate the dataset into train sets and test sets by samples rather than mass spectra. Due to the closeness of the replicate features, three replicate mass spectra from the same sample source were placed in the same dataset (training set or test set) to prevent inflated accuracy. A total of 489 mass spectra collected were summarized and

m/z were aligned. And all the intensities were normalized using the signal intensity of IS. The number of occurrences of each m/z in all spectra was calculated, and those less than 326 (489*2/3) were eliminated. Subsequently, the matrix background was checked and tested 30 times in parallel, and the m/z features with the top eight highest abundance were eliminated, and then 551 and 441 m/z features of urine and serum samples were obtained respectively, which were used as a basis for subsequent statistical analysis. Unless otherwise stated, data were acquired from at least three independent experiments. Machine learning (ML) was carried out with the Orange 3.31.1 module in Python 3.7. The build-in classifier neural network (NN), random forest (RF), logistic regression (LR), naive bayes (NB), support vector machine (SVM), adaboost (AB) and k-nearest neighbor (kNN) were applied and evaluated by leave one out cross-validation, and build-in FreeViz was used for data visualization. The accuracy, specificity, F1, precision and recall combined with the visualized receiver operating characteristic (ROC) curve were used to evaluate the classification model. Model parameters were set as follows: NN: Hidden layers: 100, Activation: ReLu, Solver: Adam, Alpha: 0.0001, Max iterations: 200, Replicable training: True. RF: Number of trees: 10, Maximal number of considered features: unlimited, Replicable training: No, Maximal tree depth: unlimited, Stop splitting nodes with maximum instances: 5. LR: Regularization: Ridge (L2), C=1, class weights=False. NB: No additional parameter settings are performed. SVM: SVM type: SVM, C=1.0, ε=0.1, Kernel: RBF, $\exp(-\text{auto}|x-y|^2)$, Numerical tolerance: 0.001, Iteration limt: 100. AB: Base estimator: tree, Number of estimators: 50, Algorithm (classification): Samme.r, Loss (regression): Linear. kNN: Number of neighbours: 5, Metric: Euclidean, Weight: Uniform. The confusion matrix and violin diagram were drawn by Origin 2022. The principal component analysis (PCA), partial least squares discriminant analysis (PLS-DA), sparse partial least squares discriminant analysis (sPLS-DA) and orthogonal partial least squares discriminant analysis (OPLS-DA) were performed using the MetaboAnalyst 5.0 at https://www.metaboanalyst.ca/. The heatmap and clustering correlation heatmap with signs were performed using the OmicStudio tools at https://www.omicstudio.cn/.

Discrimination between individual ADs (RA, SLE, AS, SS, excepting SSc and CTD with small sample sizes) and HC were conducted. Imbalanced class designs will have an impact on the performance of the classifier. Therefore, a down-sampling scheme was applied to account for differences in the number of participants between the groups. In each pairwise analysis, the dominant class was randomly subsampled (without replacement) to the same scale as the minority class. Generally, pairwise models of RA vs HC, SLE vs HC, AS vs HC, and SS vs HC exhibited high classification accuracy for both urine and serum (AUC of 0.952 - 0.998 and accuracy of 90.5% - 97.9 % for NN, Tables S10 and S11). ROC curves and confusion matrix for NN were shown in Figure S14. FreeViz is an intelligent multivariate visualization approach[1]. Classification diagrams obtained from FreeViz were shown in Figure S15. MALDI-MS could provide important clues for potential small-molecule biomarkers. In each pairwise model of AD vs HC, top 10 discriminative m/z features were selected by FreeViz, respectively. The violin plot features were generated for visualization of the distribution differences among four types of ADs as well as HC (Figure S16)[2]. The

above results suggested that there were significant metabolic differences between diseased and healthy samples.

On account of the high number of patients with RA, it is critical to differentiate various ADs from RA. Machine learning classifiers mentioned above were conducted to distinguish the pairwise models. For SLE vs RA, AS vs RA and SS vs RA, NN achieved prominent discrimination in both urine and serum samples. Afterwards, we put the samples of 5 diseases (SLE, AS, SS, SSc and CTD) together to form the other diseases (OT) group, which was carried out for the classification with RA. NN enabled an AUC score of 0.956 and accuracy of 88.5% in urine samples, while AUC of 0.863 and accuracy of 77.4% in serum samples. However, when came to the classification model of OT (5) vs RA vs HC, the AUC and accuracy were raised to 0.947 and 83.2% of NN in serum samples. As for the classification model among four diseases SS vs AS vs SLE vs RA, the AUC and accuracy of NN in serum samples only reached 0.873 and 67.9%, respectively. Meanwhile, excellent classification results were obtained for all models in urine samples by NN (Figure S17, Tables S12 and S13).

Author contributions

Z.N. planned and designed this work, and developed the overall approach. Q.D. performed the experiments and wrote the manuscript. H.L. optimized the experimental protocols. L.J., W.L. and J.L. helped with sample collection. X.W. and J.C. contributed to the data analysis. C.X. helped complete the experiments. All authors joined in the critical discussion and edited the manuscript.

Conflict of interest

The authors declare that they have no known competing financial interests or personal relationships that could have appeared to influence the work reported in this paper.

Acknowledgements

This work was supported by grants from the National Natural Science Foundation of China (Grant Nos. 21625504, 21827807, and 21790390/21790392), the Chinese Academy of Sciences and Shenzhen Science and Technology Innovation Commission (Grant No. JCYJ20210324115601005).

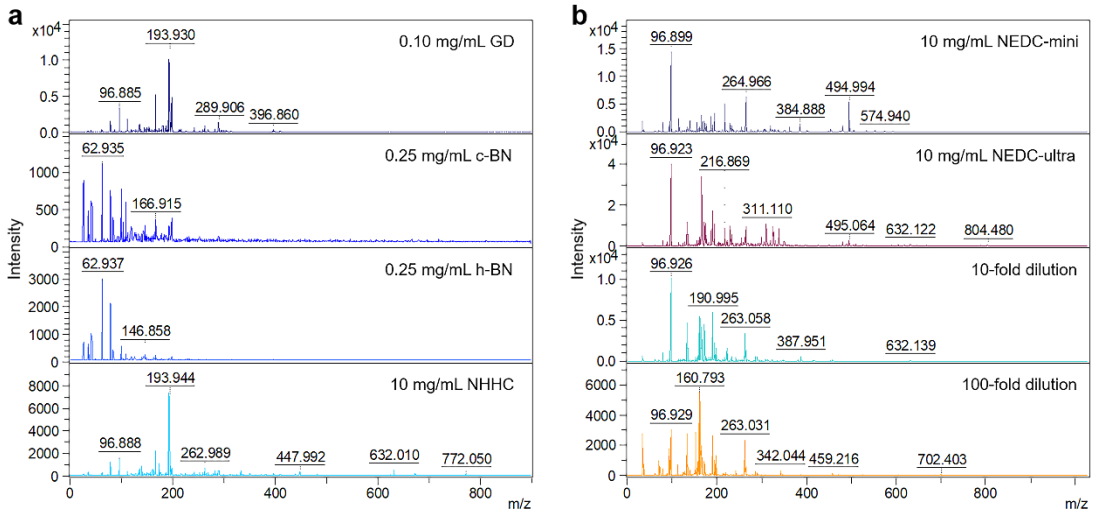

Fig. S1 Mass spectra of urine samples by MALDI-MS. **a** 0.01 mg/mL GD, 0.25 mg/mL c-BN, 0.25 mg/mL h-BN and 10 mg/mL NHHC were used as matrices. **b** 10 mg/mL NEDC was used as matrix in different spot sizes (minimum and ultra) of laser, and urine samples were diluted 10-fold and 100-fold.

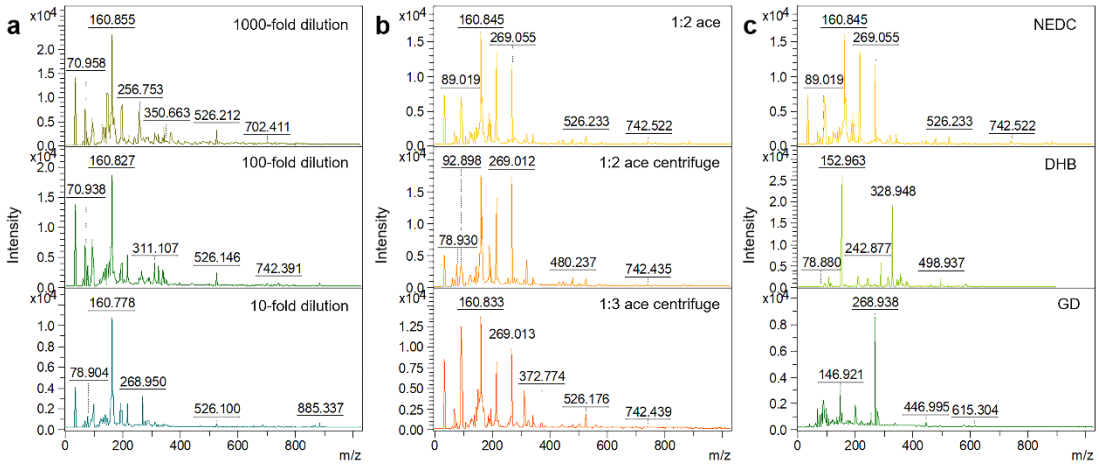

Fig. S2 Mass spectra of serum samples by MALDI-MS. **a** Serum samples were diluted 1000-fold, 100-fold and 10-fold. **b** Acetonitrile was added at a ratio of 1:2, centrifugation was conducted after acetonitrile was added at a ratio of 1:2 and 1:3. **c** NEDC, DHB and GD were used as matrices.

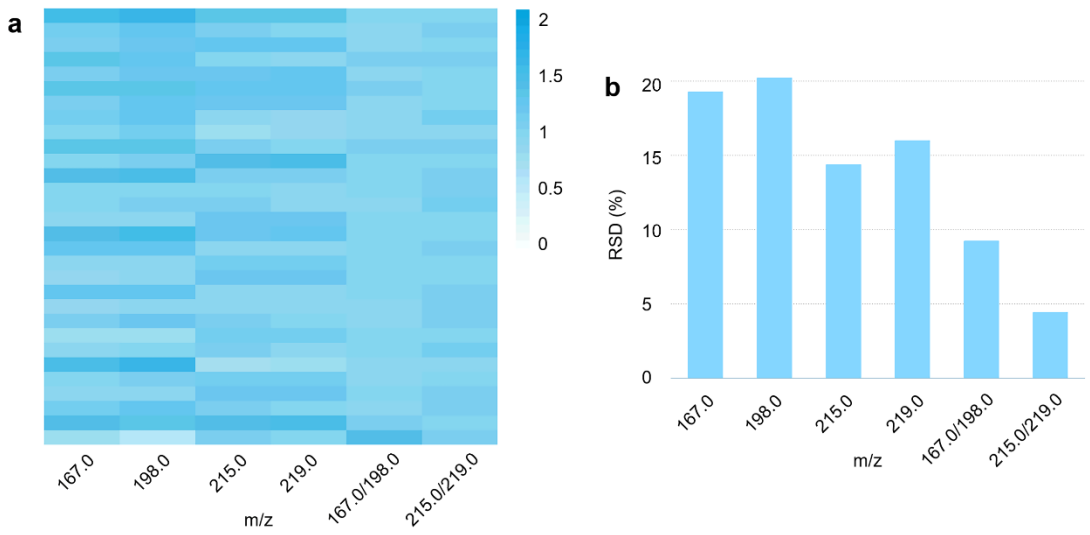

Fig. S3 The relatively quantitative ability of internal standard. **a** Repeatability heatmap of uric acid, 3-chloro-L-phenylalanine, glucose and D-glucose-1,2-$^{13}C_2$ signal intensities. **b** The relative standard deviation (RSD) of signal intensities. m/z 167.0: $[M-H]^-$ of uric acid, m/z 198.0: $[M-H]^-$ of 3-chloro-L-phenylalanine, m/z 215.0: [glucose+^{35}Cl]$^-$, m/z 219.0: [D-glucose-1,2-$^{13}C_2$+^{37}Cl]$^-$. This experiment was repeated 30 times.

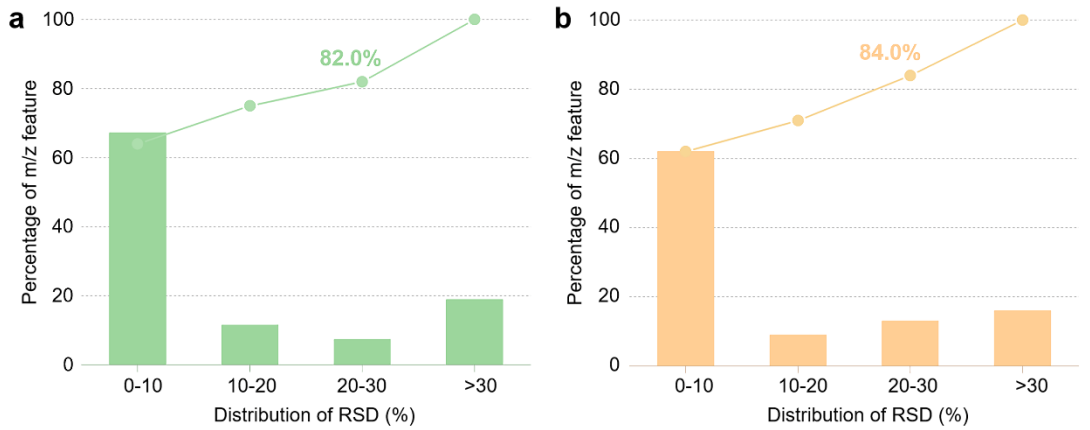

Fig. S4 RSD distributions of m/z features in urine (a) and serum (b) samples.

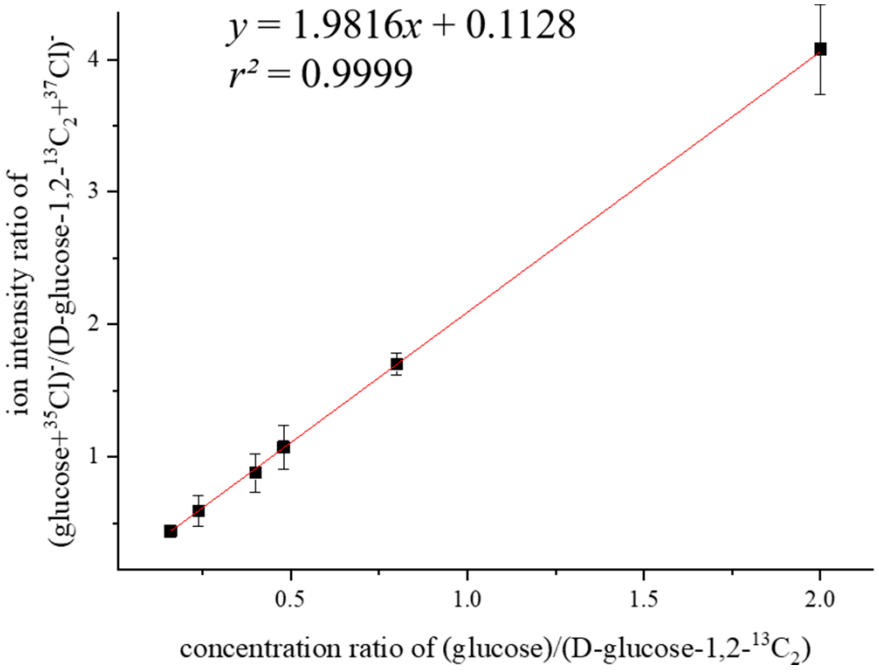

Fig. S5 Quantitative curve of glucose using D-glucose-1,2-$^{13}C_2$ as internal standard.

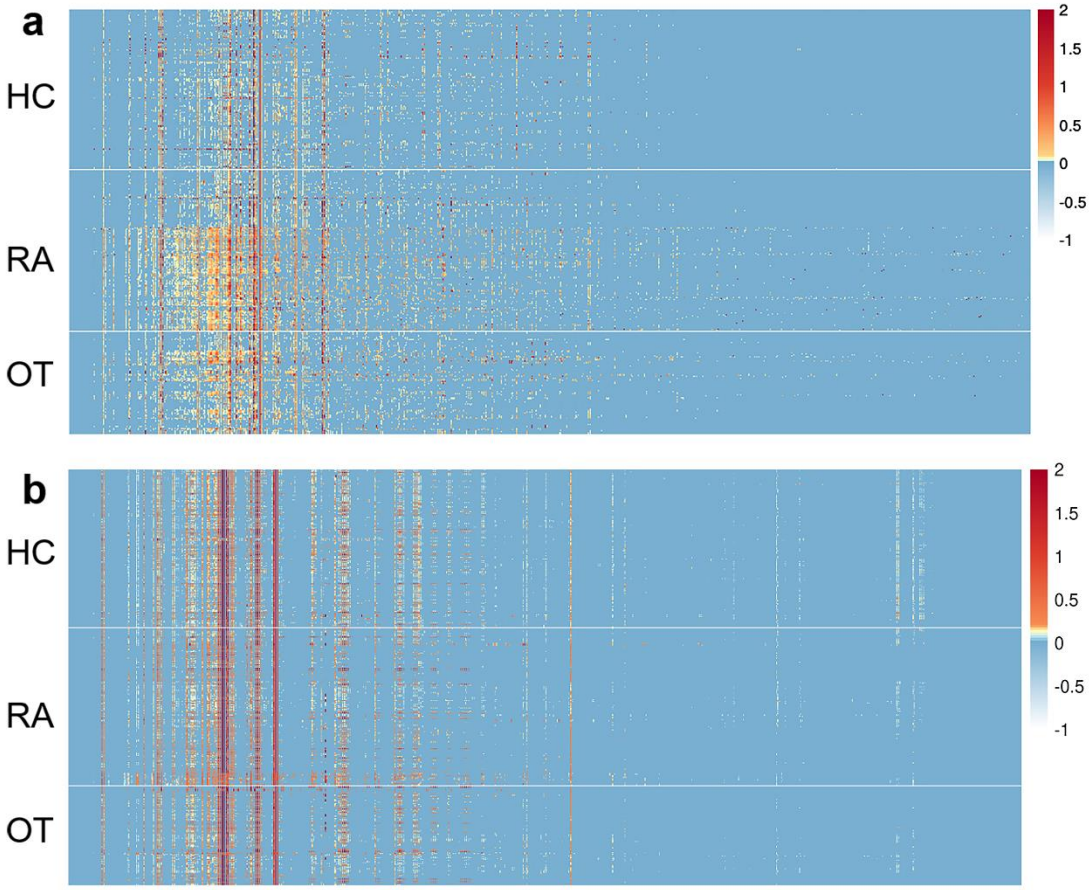

Fig. S6 Heatmaps of 489 spectra. **a** 551 m/z features for urine samples. **b** 441 m/z features for serum samples. HC (healthy controls), RA (rheumatoid arthritis), OT (other autoimmune diseases).

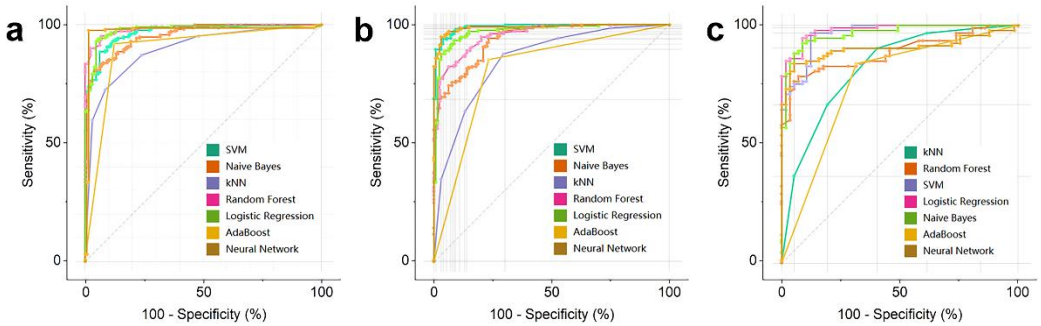

Fig. S7 ROC curves for discrimination of autoimmune diseases (ADs) from healthy controls (HC). **a** ROC curves for training cohort with urine samples. **b** ROC curves for training cohort with serum samples. **c** ROC curves for testing cohort with serum samples.

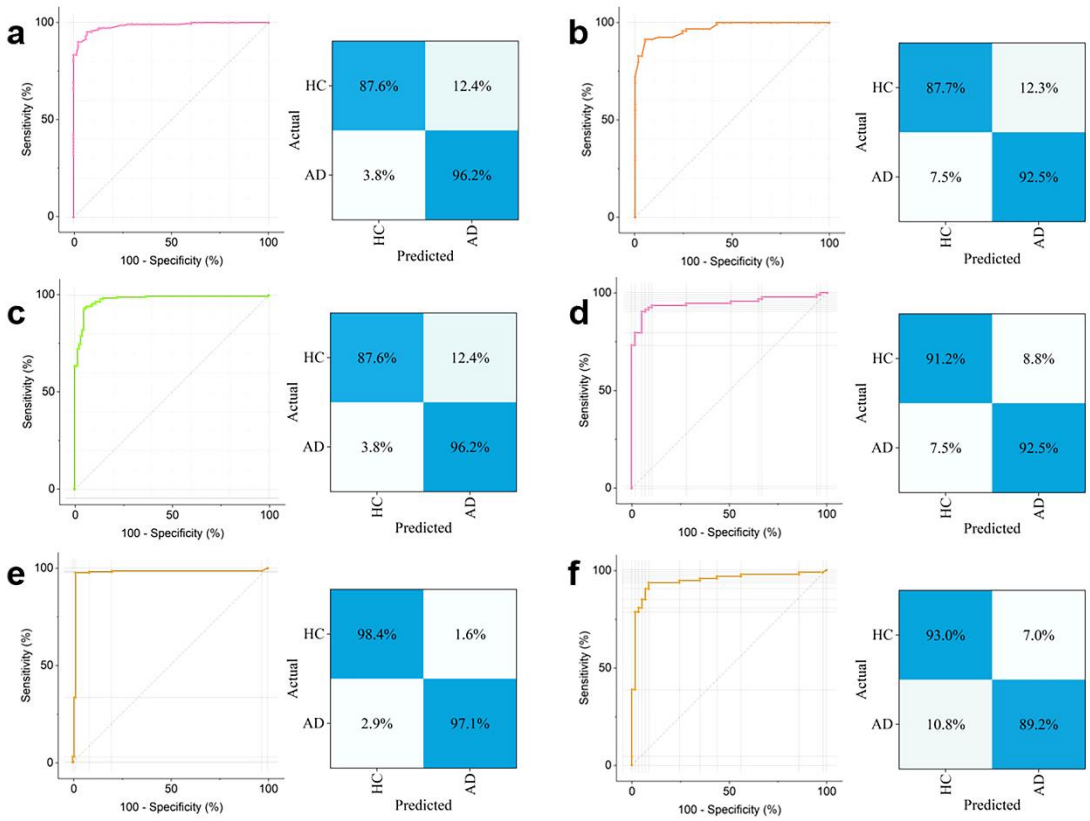

Fig. S8 ROC curve and confusion matrix for the discrimination of autoimmune diseases (ADs) from healthy controls (HC) with urine samples. **a** Random forest (RF) for training cohort. **b** RF for testing cohort. **c** Logistic regression (LR) for training cohort. **d** LR for testing cohort. **e** Neural network (NN) for training cohort. **f** NN for testing cohort.

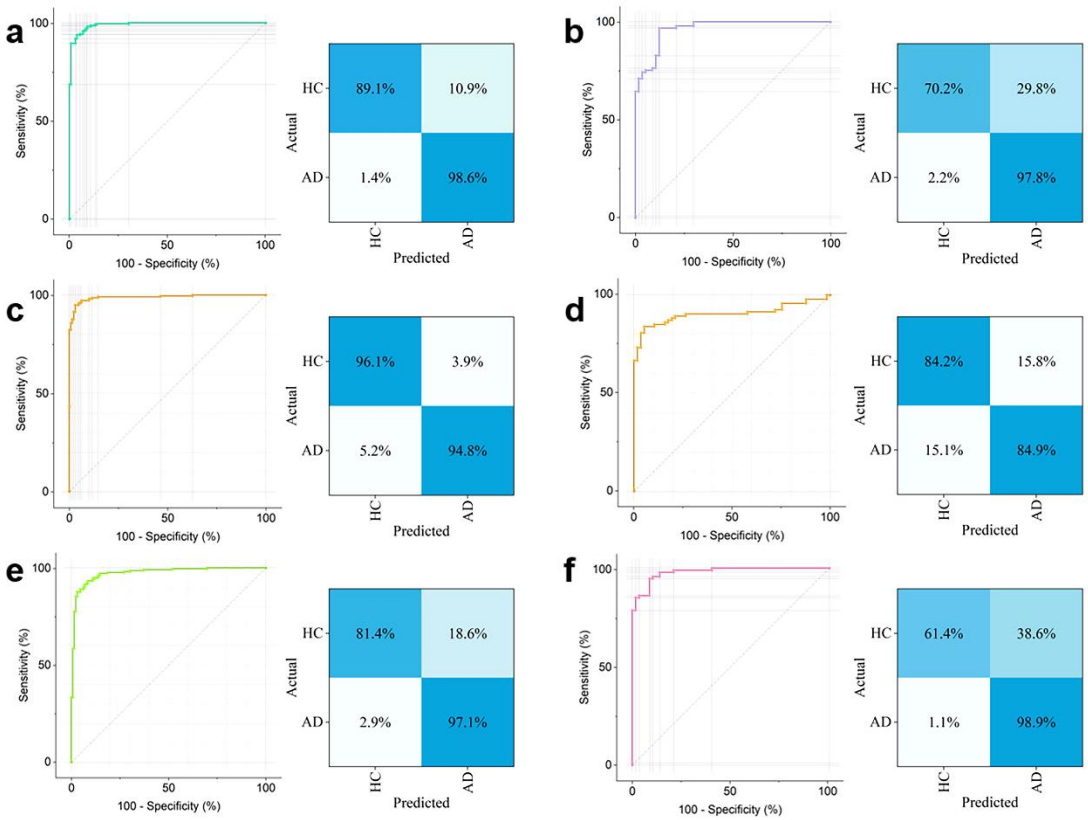

Fig. S9 ROC curve and confusion matrix for the discrimination of autoimmune diseases (ADs) from healthy controls (HC) with serum samples. **a** Support vector machine (SVM) for training cohort. **b** SVM for testing cohort. **c** Neural network (NN) for training cohort. **d** NN for testing cohort. **e** Logistic regression (LR) for training cohort. **f** LR for testing cohort.

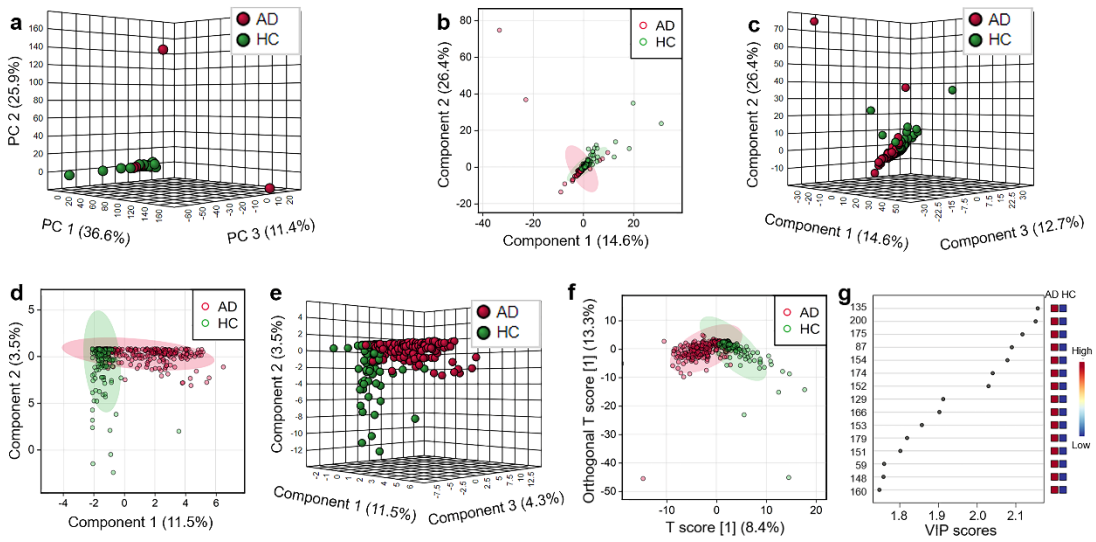

Fig. S10 Classification results of autoimmune diseases (ADs) versus healthy controls (HC) with urine samples. **a** 3D score plot of principal component analysis (PCA). **b** 2D score plot of partial least squares discriminant analysis (PLS-DA). **c** 3D score plot of PLS-DA. **d** 2D score plot of sparse partial least squares discriminant analysis (sPLS-DA). **e** 3D score plot of sPLS-DA. **f** Score plot of orthogonal partial least squares discriminant analysis (OPLS-DA). **g** Score plot of variable importance in the projection (VIP).

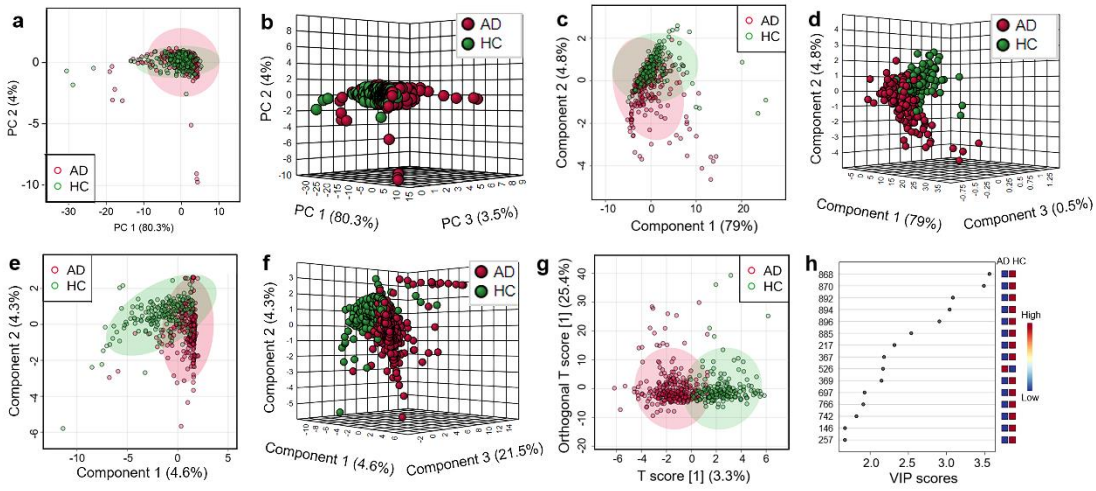

Fig. S11 Classification results of autoimmune diseases (ADs) versus healthy controls (HC) with serum samples. **a** 2D score plot of principal component analysis (PCA). **b** 3D score plot of PCA. **c** 2D score plot of partial least squares discriminant analysis (PLS-DA). **d** 3D score plot of PLS-DA. **e** 2D score plot of sparse partial least squares discriminant analysis (sPLS-DA). **f** 3D score plot of sPLS-DA. **g** Score plot of orthogonal partial least squares discriminant analysis (OPLS-DA). **h** Score plot of variable importance in the projection (VIP).

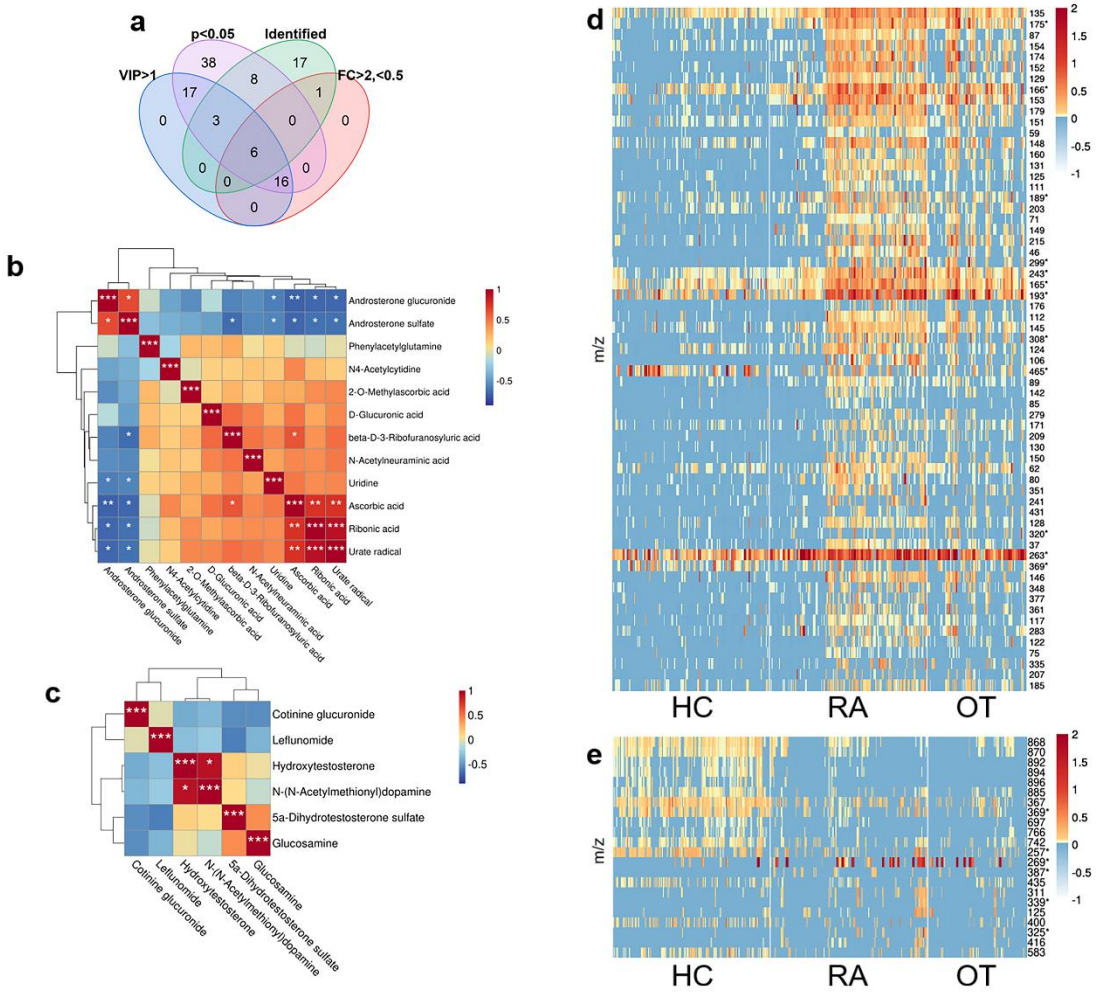

Fig. S12 Metabolic features in autoimmune diseases versus healthy controls (ADs vs HC). a Venn diagram of metabolomic features in serum samples. 22 key features were selected with $p < 0.05$, VIP > 1, fold change (FC) > 2 or < 0.5, and 6 of them were identified. b Pearson correlation heatmap of 12 differential metabolites in urine samples, c 6 differential metabolites in serum samples. Red indicated positive correlation, while blue indicated negative correlation. *: <0.05, **: <0.01, ***: <0.001. d Heatmap of the key features in urine samples, e in serum samples, * represented identified metabolites, each cell reported a relative intensity value with corresponding color, HC (healthy controls), RA (rheumatoid arthritis), OT (other autoimmune diseases).

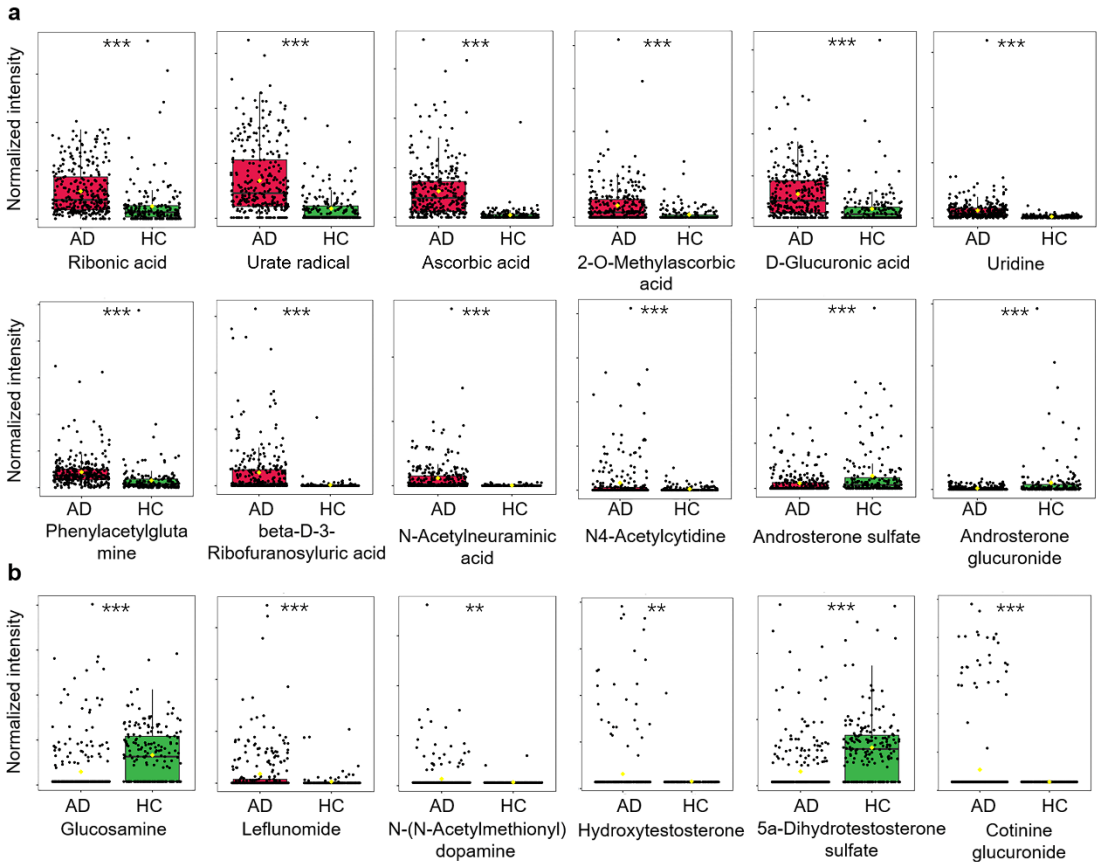

Fig. S13 Boxplots of differential metabolites between autoimmune diseases and healthy controls (ADs vs HC). a 12 differential metabolites in urine samples, b 6 differential metabolites in serum samples. (The black dots represent the concentrations of the selected feature from all samples. The notch indicates the 95% confidence interval around the median of each group, defined as +/- 1.58*IQR/sqrt(n). The notch can be used to evaluate differences between groups; if the notches do not overlap, the medians are likely different. Meanwhile, the mean concentration of each group is indicated with a yellow diamond. The FDR corrected p-value was obtained from the two-tail t-test of each metabolite between ADs and HC, and the significance of comparisons was set at *$p < 0.05$, **$p < 0.01$, and ***$p < 0.001$.)

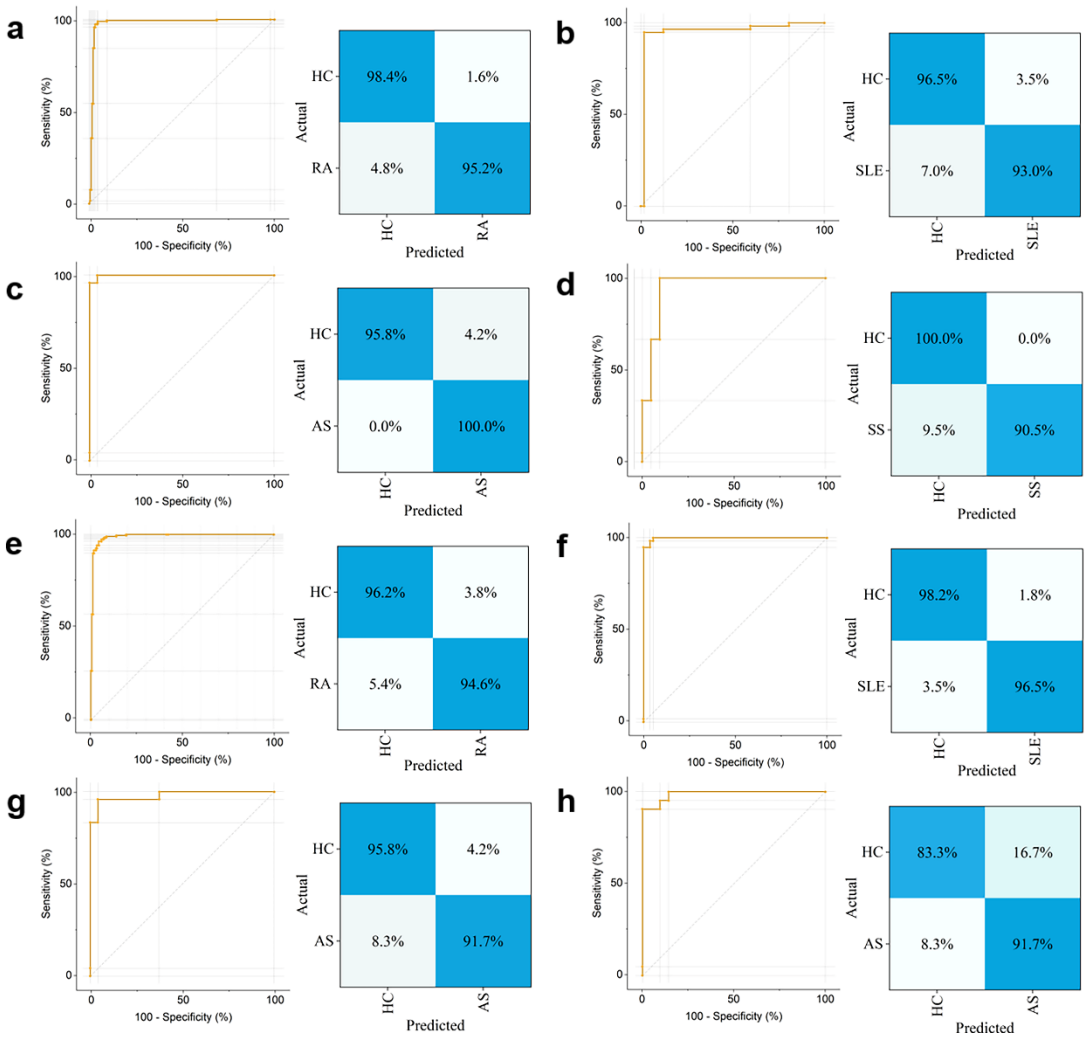

Fig. S14 ROC curve and confusion matrix for individual autoimmune diseases (ADs) versus healthy controls (HC) obtained by neural network (NN). **a** Rheumatoid arthritis (RA) vs HC, **b** systemic lupus erythematosus (SLE) vs HC, **c** ankylosing spondylitis (AS) vs HC, **d** sicca syndrome (SS) vs HC with urine samples. **e** RA vs HC, **f** SLE vs HC, **g** AS vs HC, **h** SS vs HC with serum samples.

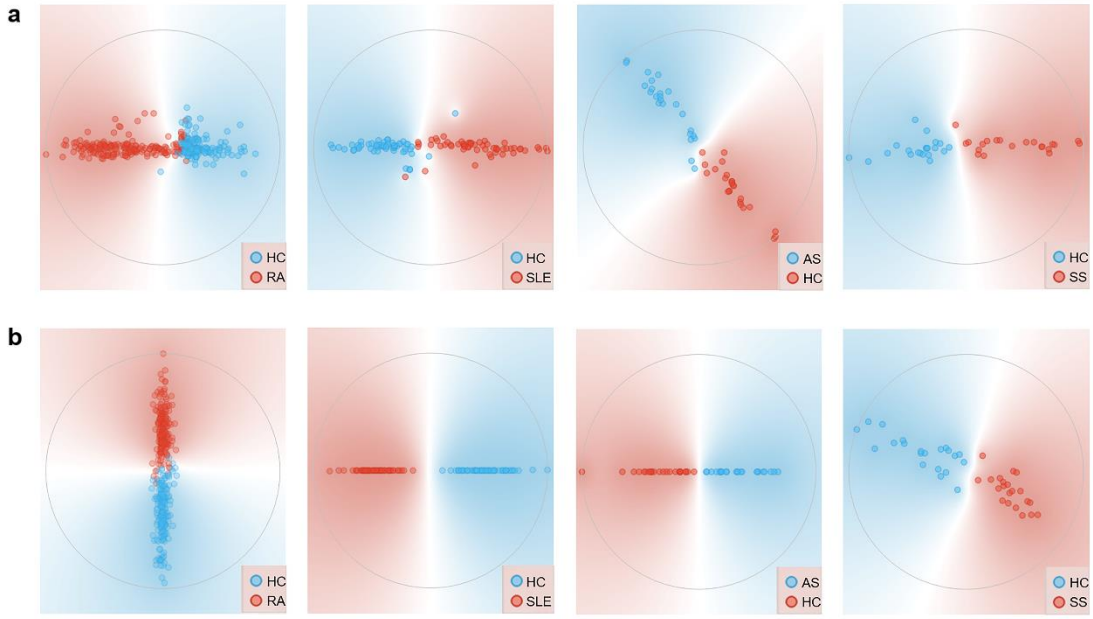

Fig. S15 Classification diagrams obtained from FreeViz of individual autoimmune diseases (ADs) versus healthy controls (HC). **a** Rheumatoid arthritis (RA) vs HC, systemic lupus erythematosus (SLE) vs HC, ankylosing spondylitis (AS) vs HC and sicca syndrome (SS) vs HC in urine samples. **b** RA vs HC, SLE vs HC, AS vs HC and SS vs HC in serum samples.

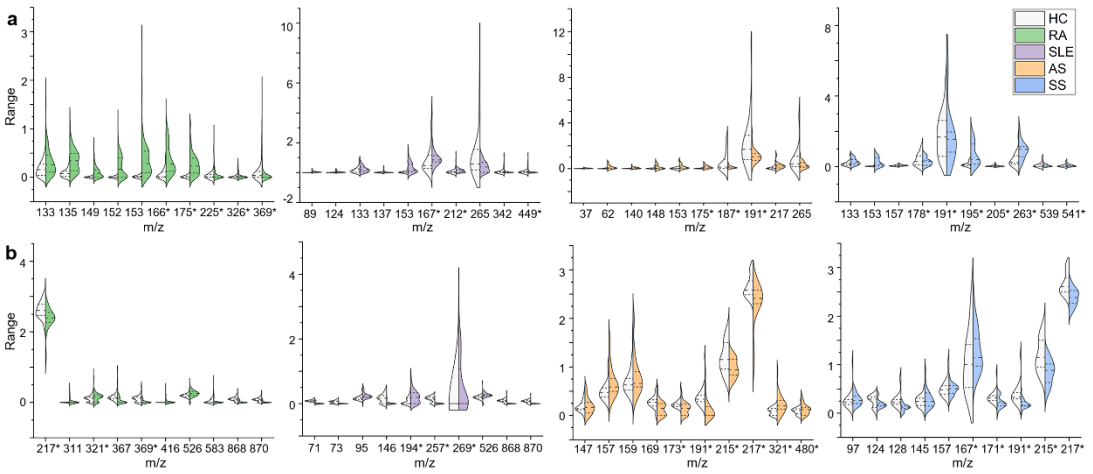

Fig. S16 Discriminating features of each autoimmune diseases (ADs) type versus healthy controls (HC). Violin plots of top 10 m/z discriminating features intensity distributions of each ADs type vs HC (The middle dash lines indicated median value of the intensities of each corresponding m/z while the upper and lower dotted lines indicated intensity values of first quartile and third quartile. Gray represented HC while the colored represented ADs). a Rheumatoid arthritis (RA) vs HC, systemic lupus erythematosus (SLE) vs HC, ankylosing spondylitis (AS) vs HC and sicca syndrome (SS) vs HC in urine samples, b RA vs HC, SLE vs HC, AS vs HC and SS vs HC in serum samples, * represented identified metabolites.

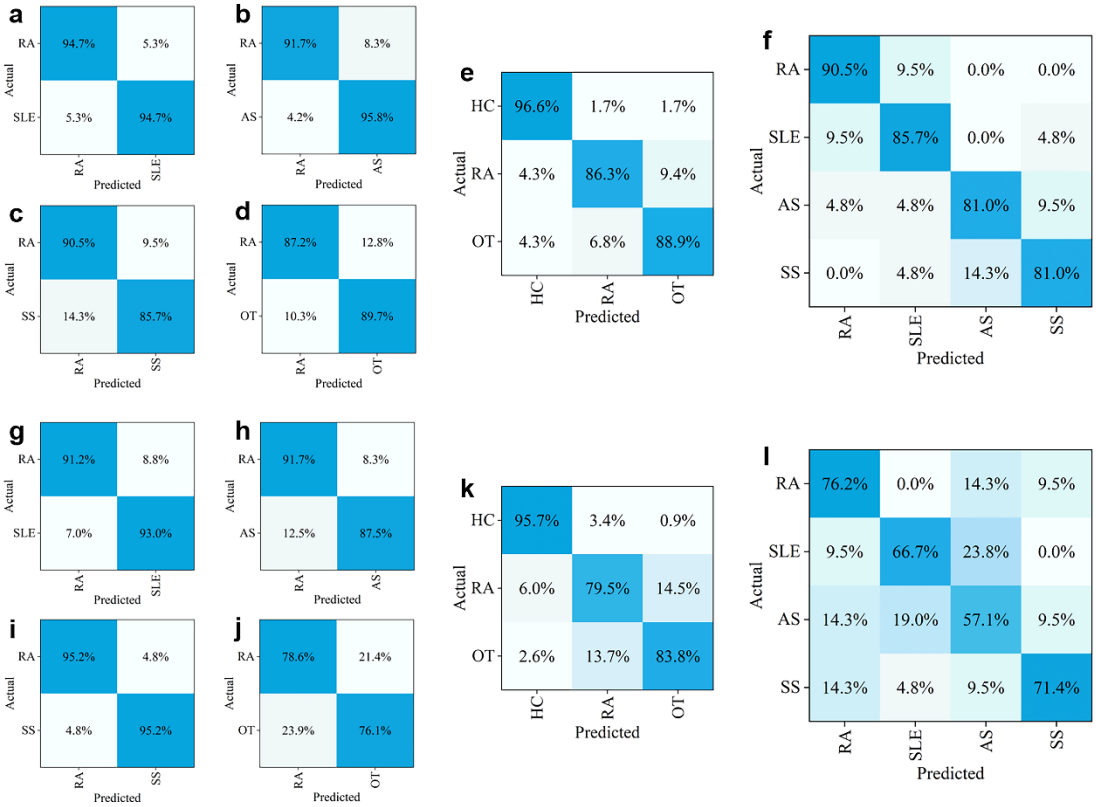

Fig. S17 Confusion matrix for different classification models. **a** Systemic lupus erythematosus (SLE) vs rheumatoid arthritis (RA), **b** ankylosing spondylitis (AS) vs RA, **c** sicca syndrome (SS) vs RA, **d** other autoimmune diseases (OT) vs RA, **e** OT vs RA vs healthy controls (HC), **f** SS vs AS vs SLE vs RA in urine samples. **g** SLE vs RA, **h** AS vs RA, **i** SS vs RA, **j** OT vs RA, **k** OT vs RA vs HC, **l** SS vs AS vs SLE vs RA in serum samples.

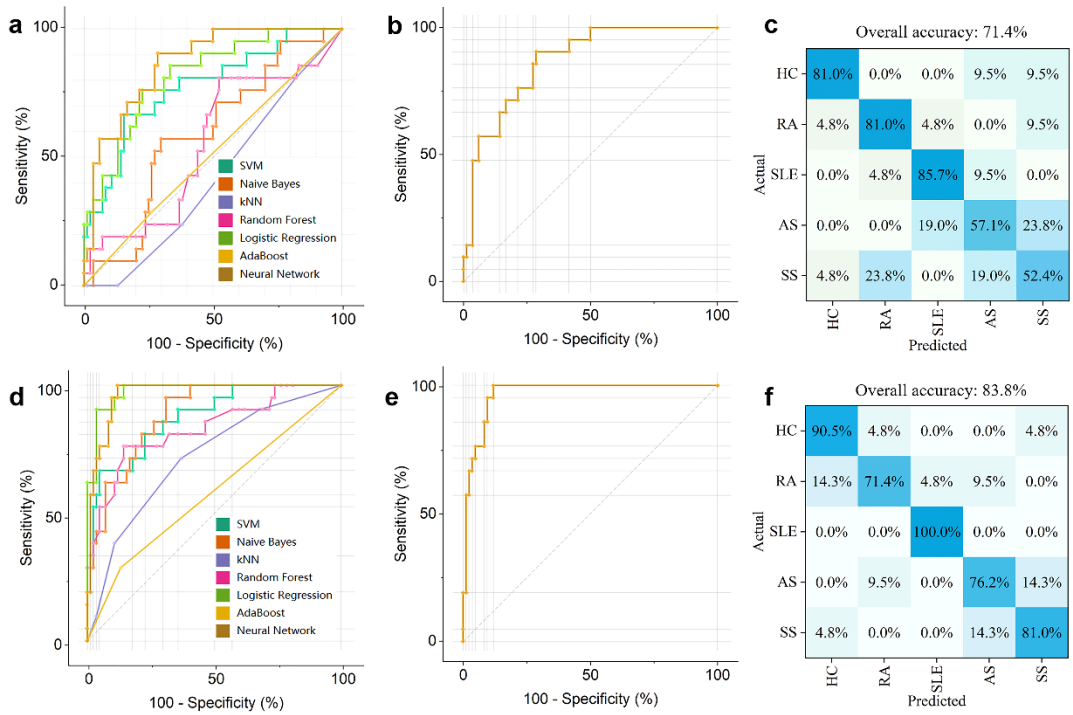

Fig. S18 Classification results of four autoimmune diseases (ADs) and healthy controls (HC). SS vs AS vs SLE vs RA vs HC, SS (sicca syndrome), AS (ankylosing spondylitis), SLE (systemic lupus erythematosus), RA (rheumatoid arthritis). a ROC curves of different classifiers in serum samples. b ROC curve of Neural Network in serum samples. c Confusion matrix of Neural Network in serum samples. d ROC curves of different classifiers in fusion model. e ROC curve of Neural Network in fusion model. f Confusion matrix of Neural Network in fusion model.

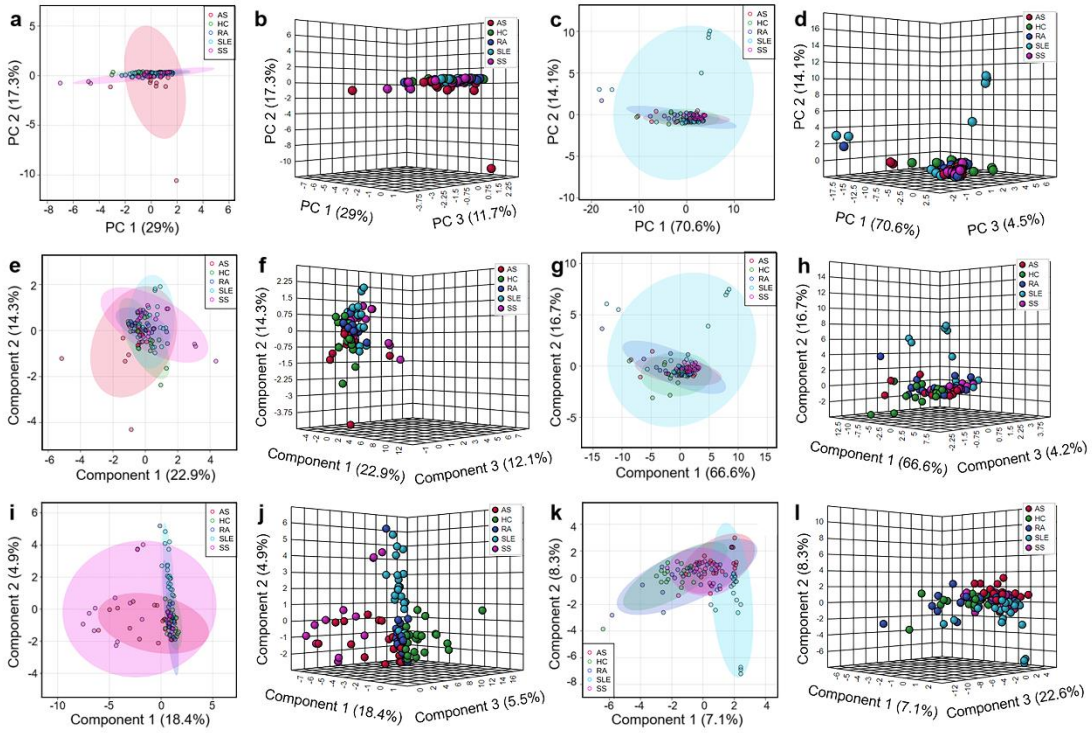

Fig. S19 Classification results of four autoimmune diseases (ADs) and healthy controls (HC). SS vs AS vs SLE vs RA vs HC, SS (sicca syndrome), AS (ankylosing spondylitis), SLE (systemic lupus erythematosus), RA (rheumatoid arthritis). **a** 2D score plot of principal component analysis (PCA) in urine samples. **b** 3D score plot of PCA in urine samples. **c** 2D score plot of PCA in serum samples. **d** 3D score plot of PCA in serum samples. **e** 2D score plot of partial least squares discriminant analysis (PLS-DA) in urine samples. **f** 3D score plot of PLS-DA in urine samples. **g** 2D score plot of PLS-DA in serum samples. **h** 3D score plot of PLS-DA in serum samples. **i** 2D score plot of sparse partial least squares discriminant analysis (sPLS-DA) in urine samples. **j** 3D score plot of sPLS-DA in urine samples. **k** 2D score plot of sPLS-DA in serum samples. **l** 3D score plot of sPLS-DA in serum samples.

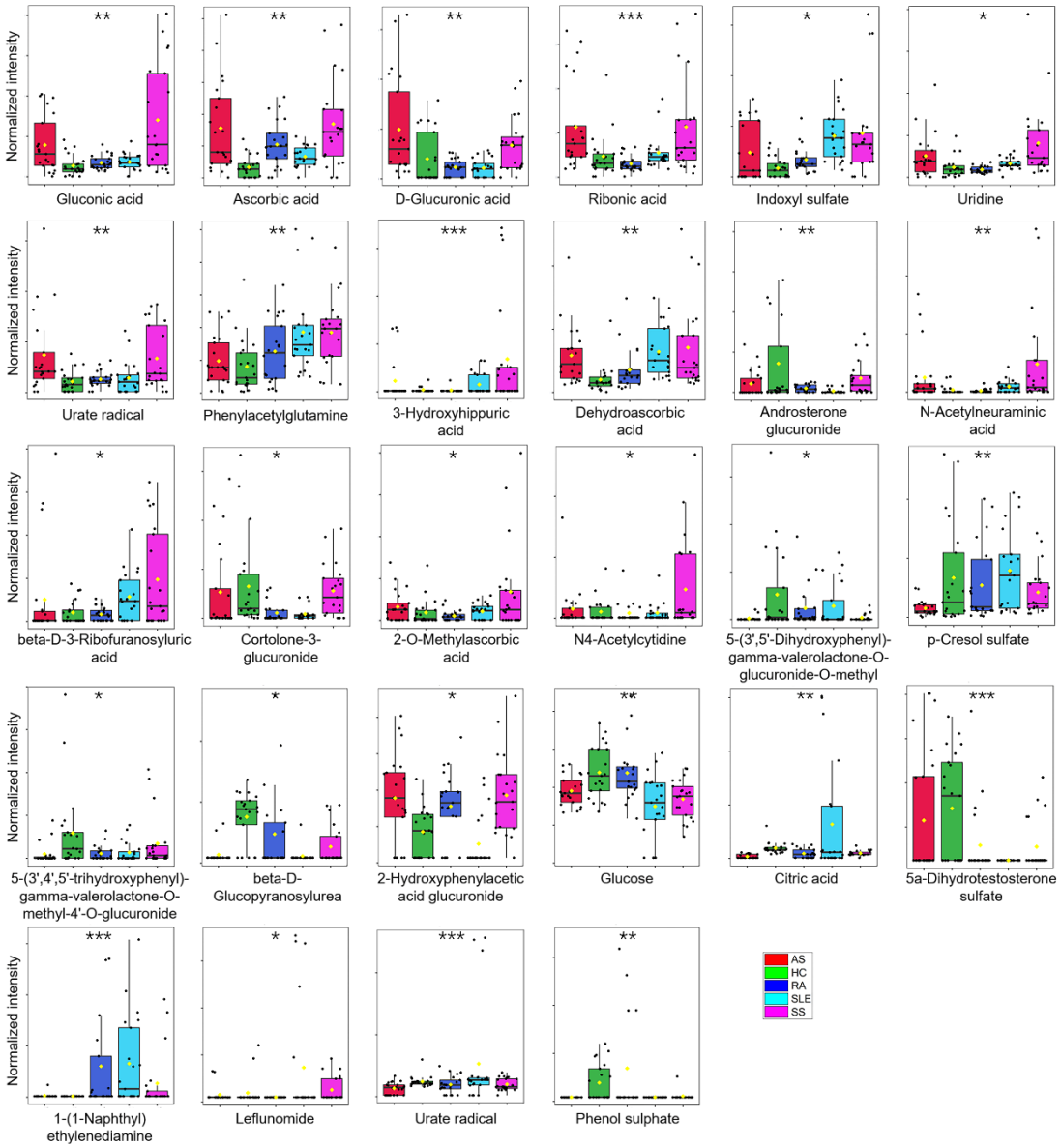

Fig. S20 Boxplots of characteristic metabolites in the distinction of four autoimmune diseases (ADs) and healthy controls (HC). SS vs AS vs SLE vs RA vs HC, SS (sicca syndrome), AS (ankylosing spondylitis), SLE (systemic lupus erythematosus), RA (rheumatoid arthritis). 19 characteristic metabolites in urine samples and 9 characteristic metabolites in serum samples. (The black dots represent the concentrations of the selected feature from all samples. The notch indicates the 95% confidence interval around the median of each group, defined as +/- 1.58*IQR/ sqrt(n). The notch can be used to evaluate differences between groups; if the notches do not overlap, the medians are likely different. Meanwhile, the mean concentration of each group is indicated with a yellow diamond. The FDR corrected p-value was obtained from the one-way analysis of variance (ANOVA) of each metabolite between four ADs and HC, and the significance of comparisons was set at *$p < 0.05$, **$p < 0.01$, and ***$p < 0.001$.)

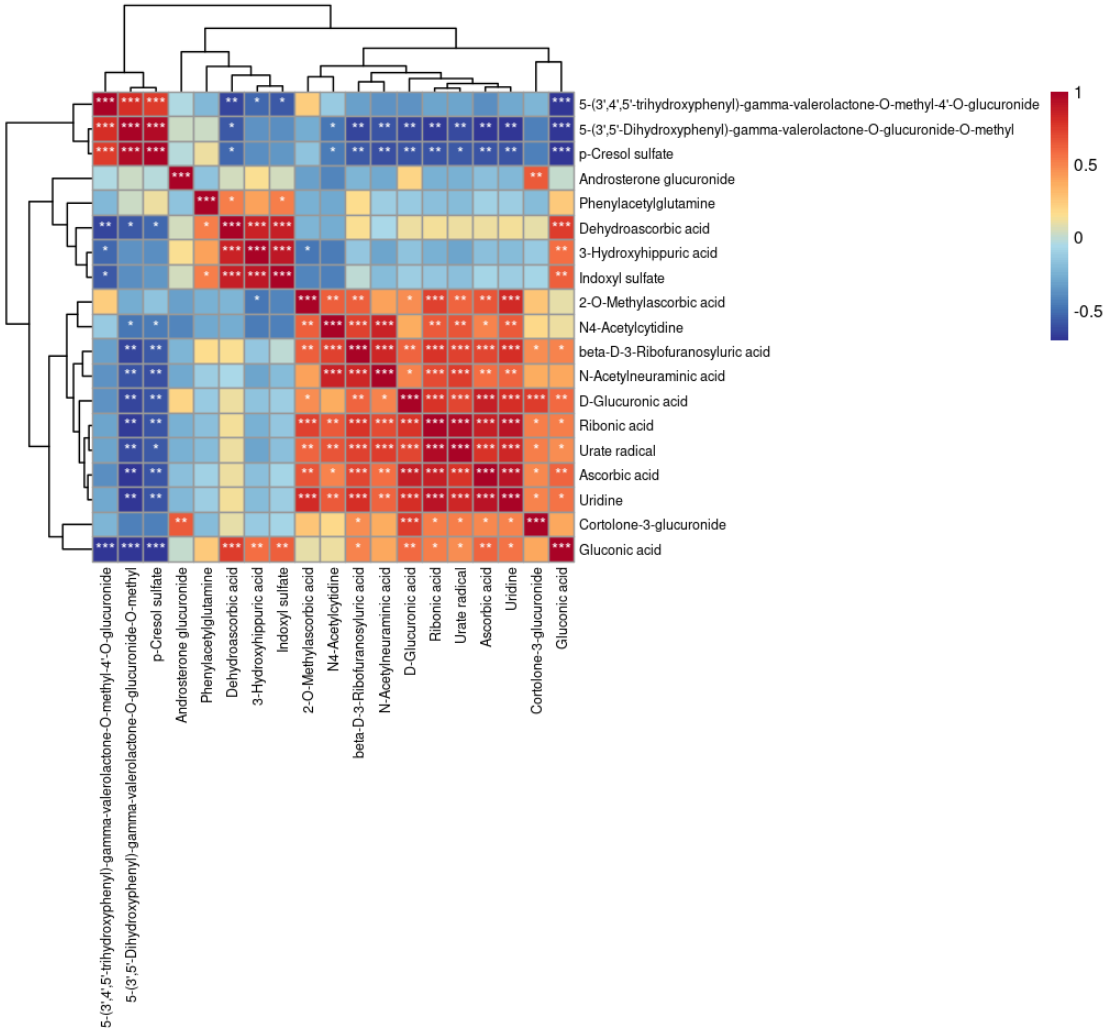

Fig. S21 Pearson correlation heatmap of 19 characteristic metabolites in the distinction of four autoimmune diseases (ADs) and healthy controls (HC) in urine samples. Red indicated positive correlation, while blue indicated negative correlation. *: <0.05, **: <0.01, ***: <0.001.

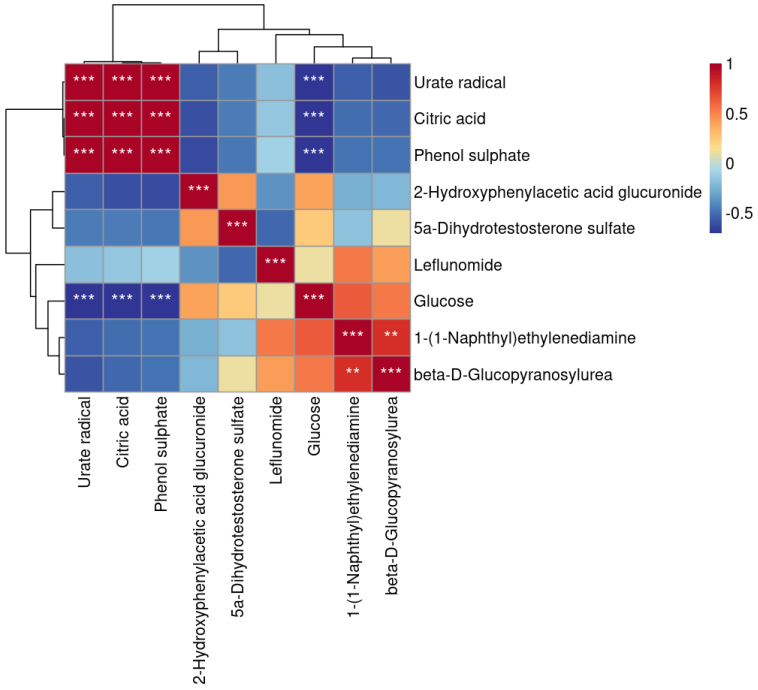

Fig. S22 Pearson correlation heatmap of 9 characteristic metabolites in the distinction of four autoimmune diseases (ADs) and healthy controls (HC) in serum samples. Red indicated positive correlation, while blue indicated negative correlation. *: <0.05, **: <0.01, ***: <0.001.

Table S1 Age and gender distribution of study participants.

Groups	Number	Age						Gender	
		< 30	30-39	40-49	50-59	60-69	≥70	Male	Female
Healthy controls	62	8	5	14	19	8	8	28	34
Autoimmune diseases	101	10	9	17	36	15	14	32	69

Table S2 Metrics of classifiers for autoimmune diseases versus healthy controls (ADs vs HC) with urine samples (training cohort).

Model	AUC	Accuracy	F1	Precision	Recall
Random Forest	0.983	0.929	0.929	0.929	0.929
Logistic Regression	0.977	0.935	0.935	0.935	0.935
Neural Network	0.972	0.976	0.976	0.977	0.976
Support Vector Machine	0.966	0.900	0.901	0.907	0.900
Naive Bayes	0.955	0.820	0.822	0.871	0.820
AdaBoost	0.898	0.903	0.903	0.903	0.903
k-Nearest Neighbor	0.896	0.829	0.828	0.828	0.829

Table S3 Metrics of classifiers for autoimmune diseases versus healthy controls (ADs vs HC) with urine samples (testing cohort).

Model	AUC	Accuracy	F1	Precision	Recall
Random Forest	0.970	0.907	0.907	0.907	0.907
Support Vector Machine	0.960	0.873	0.875	0.882	0.873
Logistic Regression	0.947	0.920	0.920	0.921	0.920
Neural Network	0.946	0.907	0.907	0.911	0.907
Naive Bayes	0.942	0.873	0.875	0.882	0.873
k-Nearest Neighbor	0.887	0.787	0.783	0.784	0.787
AdaBoost	0.834	0.840	0.841	0.841	0.840

Table S4 Metrics of classifiers for autoimmune diseases versus healthy controls (ADs vs HC) with serum samples (training cohort).

Model	AUC	Accuracy	F1	Precision	Recall
Support Vector Machine	0.990	0.950	0.949	0.951	0.950
Neural Network	0.989	0.953	0.953	0.954	0.953
Logistic Regression	0.973	0.912	0.910	0.914	0.912
Random Forest	0.956	0.879	0.878	0.878	0.879
Naive Bayes	0.940	0.826	0.827	0.830	0.826
k-Nearest Neighbor	0.852	0.811	0.809	0.809	0.811
AdaBoost	0.810	0.820	0.820	0.820	0.820

Table S5 Metrics of classifiers for autoimmune diseases versus healthy controls (ADs vs HC) with serum samples (testing cohort).

Model	AUC	Accuracy	F1	Precision	Recall
Logistic Regression	0.980	0.847	0.837	0.870	0.847
Naive Bayes	0.966	0.907	0.906	0.907	0.907
Support Vector Machine	0.964	0.873	0.868	0.884	0.873
Neural Network	0.904	0.847	0.848	0.851	0.847
Random Forest	0.887	0.787	0.787	0.787	0.787
k-Nearest Neighbor	0.824	0.787	0.779	0.787	0.787
AdaBoost	0.761	0.780	0.779	0.778	0.780

Table S6 Metabolites identified in urine samples in negative ion mode.

Experimental m/z	Theoretical m/z	Delta (ppm)	Formula	Adduct	Compound Name	Identification Database
165.04053	165.04046	0.42414	$C_5H_{10}O_6$	$[M-H]^-$	Ribonic acid*†‡	HMDB0000867
166.01326	166.01324	0.12047	$C_5H_3N_4O_3$	$[M-H]^-$	Urate radical*†‡	HMDB0060260
167.02109	167.02106	0.17962	$C_5H_4N_4O_3$	$[M-H]^-$	Uric acid*	HMDB0000289
172.99143	172.99140	0.17342	$C_6H_6O_4S$	$[M-H]^-$	Phenol sulphate*	HMDB0060015
173.00919	173.00916	0.17340	$C_6H_6O_6$	$[M-H]^-$	Dehydroascorbic acid*‡	HMDB0001264
173.00919	173.00916	0.17340	$C_6H_6O_6$	$[M-H]^-$	Aconitic acid*	HMDB0247961
175.02481	175.02481	0.00000	$C_6H_8O_6$	$[M-H]^-$	Ascorbic acid*†‡	HMDB0000044
178.05098	178.05097	0.05616	$C_9H_9NO_3$	$[M-H]^-$	Hippuric acid*	HMDB0000714
187.00707	187.00705	0.10695	$C_7H_8O_4S$	$[M-H]^-$	p-Cresol sulfate*‡	HMDB0011635
189.04048	189.04046	0.10580	$C_7H_{10}O_6$	$[M-H]^-$	2-O-Methylascorbic acid*†‡	HMDB0240294
191.01974	191.01973	0.05235	$C_6H_8O_7$	$[M-H]^-$	Citric acid*	HMDB0000094
193.03537	193.03538	0.05180	$C_6H_{10}O_7$	$[M-H]^-$	D-Glucuronic acid*†‡	HMDB0000127
194.04588	194.04588	0.00000	$C_9H_9NO_4$	$[M-H]^-$	Salicyluric acid	HMDB0000840
194.04588	194.04588	0.00000	$C_9H_9NO_4$	$[M-H]^-$	3-Hydroxyhippuric acid*‡	HMDB0006116
194.04588	194.04588	0.00000	$C_9H_9NO_4$	$[M-H]^-$	4-Hydroxyhippuric acid*	HMDB0013678
195.05105	195.05103	0.10254	$C_6H_{12}O_7$	$[M-H]^-$	Gluconic acid*‡	HMDB0000625
195.05105	195.05103	0.10254	$C_6H_{12}O_7$	$[M-H]^-$	Galactonic acid	HMDB0000565
195.05236	195.05236	0.00000	$C_7H_8N_4O_3$	$[M-H]^-$	3,9-Dimethyluric acid	HMDB0059704
195.05236	195.05236	0.00000	$C_7H_8N_4O_3$	$[M-H]^-$	1,7-Dimethyluric acid*	HMDB0011103
195.05236	195.05236	0.00000	$C_7H_8N_4O_3$	$[M-H]^-$	7,9-Dimethyluric acid	HMDB0004308
195.05236	195.05236	0.00000	$C_7H_8N_4O_3$	$[M-H]^-$	1,9-Dimethyluric acid	HMDB0002026
195.05236	195.05236	0.00000	$C_7H_8N_4O_3$	$[M-H]^-$	3,7-Dimethyluric acid*	HMDB0001982
195.05236	195.05236	0.00000	$C_7H_8N_4O_3$	$[M-H]^-$	1,3-Dimethyluric acid	HMDB0001857

205.03538	205.03538	0.00000	$C_7H_{10}O_7$	$[M-H]^-$	2-Methylcitric acid	HMDB0000379
212.00232	212.00230	0.09434	$C_8H_7NO_4S$	$[M-H]^-$	Indoxyl sulfate*‡	HMDB0000682
212.00232	212.00230	0.09434	$C_8H_7NO_4S$	$[M-H]^-$	7-Hydroxyindole sulfate*	HMDB0240659
212.00232	212.00230	0.09434	$C_8H_7NO_4S$	$[M-H]^-$	6-Hydroxyindole sulfate	HMDB0240651
225.08808	225.08808	0.00000	$C_{10}H_{14}N_2O_4$	$[M-H]^-$	Porphobilinogen*	HMDB0000245
243.06224	243.06226	0.08228	$C_9H_{12}N_2O_6$	$[M-H]^-$	Uridine*†‡	HMDB0000296
243.06224	243.06226	0.08228	$C_9H_{12}N_2O_6$	$[M-H]^-$	Pseudouridine*	HMDB0000767
263.10375	263.10373	0.07602	$C_{13}H_{16}N_2O_4$	$[M-H]^-$	Phenylacetylglutamine*†‡	HMDB0006344
299.06348	299.06332	0.53500	$C_{10}H_{12}N_4O_7$	$[M-H]^-$	beta-D-3-Ribofuranosyluric acid*†‡	HMDB0029920
305.10310	305.10306	0.13110	$C_{16}H_{18}O_6$	$[M-H]^-$	6-O-Desmethyl-mycophenolic acid	HMDB0060788
308.09883	308.09871	0.38949	$C_{11}H_{19}NO_9$	$[M-H]^-$	N-Acetylneuraminic acid*†‡	HMDB0000230
320.06549	320.06549	0.00000	$C_{11}H_{15}N_3O_6$	$[M+Cl]^-$	N4-Acetylcytidine*†‡	HMDB0005923
326.08814	326.08814	0.00000	$C_{14}H_{17}NO_8$	$[M-H]^-$	Blepharin*	HMDB0029344
326.08814	326.08814	0.00000	$C_{14}H_{17}NO_8$	$[M-H]^-$	Acetaminophen glucuronide*	HMDB0010316
330.09175	330.09179	0.12118	$C_{16}H_{17}N_3O_3S$	$[M-H]^-$	(R)-2-Amino-3-benzylthio-N-(4-nitrophenyl)propionamide	HMDB0247352
330.09175	330.09179	0.12118	$C_{16}H_{17}N_3O_3S$	$[M-H]^-$	5'-O-Desmethyl omeprazole	HMDB0014011
369.17412	369.17412	0.00000	$C_{19}H_{30}O_5S$	$[M-H]^-$	Androsterone sulfate*†	HMDB0002759
397.11428	397.11402	0.65472	$C_{18}H_{22}O_{10}$	$[M-H]^-$	5-(3',5'-Dihydroxyphenyl)-gamma-valerolactone-O-glucuronide-O-methyl*‡	HMDB0060030
397.11428	397.11402	0.65472	$C_{18}H_{22}O_{10}$	$[M-H]^-$	5-(3',4'-Dihydroxyphenyl)-gamma-valerolactone-4'-O-methyl-3'-O-glucuronide	HMDB0059990
397.11428	397.11402	0.65472	$C_{18}H_{22}O_{10}$	$[M-H]^-$	5-(3',4'-Dihydroxyphenyl)-gamma-valerolactone-3'-O-methyl-4'-O-glucuronide	HMDB0059988
397.11428	397.11402	0.65472	$C_{18}H_{22}O_{10}$	$[M-H]^-$	5-(3',4'-dihydroxyphenyl)-gamma-valerolactone-3'-O-glucuronide	HMDB0029190
413.10878	413.10894	0.38731	$C_{18}H_{22}O_{11}$	$[M-H]^-$	5-(3',4',5'-trihydroxyphenyl)-gamma-valerolactone-O-methyl-4'-O-glucuronide*‡	HMDB0060027
413.10878	413.10894	0.38731	$C_{18}H_{22}O_{11}$	$[M-H]^-$	5-(3',4',5'-trihydroxyphenyl)-gamma-valerolactone-O-methyl-5'-O-glucuronide	HMDB0060028
433.13498	433.13515	0.39249	$C_{18}H_{26}O_{12}$	$[M-H]^-$	4-Hydroxy-5-(3',5'-dihydroxyphenyl)-valeric acid-O-methyl-O-glucuronide	HMDB0059974
433.13498	433.13515	0.39249	$C_{18}H_{26}O_{12}$	$[M-H]^-$	4-Hydroxy-5-(3',4'-dihydroxyphenyl)-valeric acid-O-methyl-O-glucuronide	HMDB0059972
449.25393	449.25448	1.22425	$C_{25}H_{40}O_8$	$[M-H_2O-H]^-$	17-Hydroxyandrostane-3-glucuronide*	HMDB0010359

449.25393	449.25448	1.22425	$C_{25}H_{40}O_8$	$[M-H_2O-H]^-$	3-alpha-Androstanediol glucuronide*	HMDB0010339
449.25393	449.25448	1.22425	$C_{25}H_{40}O_8$	$[M-H_2O-H]^-$	3,17-Androstanediol glucuronide*	HMDB0010321
465.24943	465.24939	0.08598	$C_{25}H_{38}O_8$	$[M-H]^-$	Androsterone glucuronide*†‡	HMDB0002829
481.13512	481.13582	1.45489	$C_{26}H_{29}ClN_2O_4S$	$[M-H_2O-H]^-$	(E)-N-(2-(((3-(4-Chlorophenyl)allyl)(methyl)amino)methyl)phenyl)-N-(2-hydroxyethyl)-4-methoxybenzenesulfonamide	HMDB0253810
495.15078	495.15080	0.04039	$C_{23}H_{28}O_{12}$	$[M-H]^-$	Mycophenolic acid glucuronide	HMDB0060634
495.15078	495.15080	0.04039	$C_{23}H_{28}O_{12}$	$[M-H]^-$	Mycophenolic acid O-acyl-glucuronide	HMDB0060491
541.26544	541.26544	0.00000	$C_{27}H_{42}O_{11}$	$[M-H]^-$	Cortolone-3-glucuronide*‡	HMDB0010320

* Metabolites validated by LC-MS/MS, † Differential metabolites in ADs vs HC, ‡ Differential metabolites in SS vs AS vs SLE vs RA vs HC.

Table S7 Metabolites identified in serum samples in negative ion mode.

Experimental m/z	Theoretical m/z	Delta (ppm)	Formula	Adduct	Compound Name	Identification Database
159.84517	159.84515	0.12512	Cl_2Mn	$[M+Cl]^-$	Manganese(II) chloride	HMDB0303438
165.00544	165.00541	0.18181	$C_5H_2N_4O_3$	$[M-H]^-$	Nitroimidazo-oxazine	HMDB0255651
166.01327	166.01324	0.18071	$C_5H_3N_4O_3$	$[M-H]^-$	Urate radical*‡	HMDB0060260
167.02109	167.02106	0.17962	$C_5H_4N_4O_3$	$[M-H]^-$	Uric acid*	HMDB0000289
167.06150	167.06147	0.17957	$C_{11}H_8N_2$	$[M-H]^-$	Pyrroloquinoline	HMDB0257007
167.06150	167.06147	0.17957	$C_{11}H_8N_2$	$[M-H]^-$	5H-Pyrido[4,3-b]indole	HMDB0247024
167.06150	167.06147	0.17957	$C_{11}H_8N_2$	$[M-H]^-$	1H-Pyrrolo[2,3-f]quinoline	HMDB0244904
167.06150	167.06147	0.17957	$C_{11}H_8N_2$	$[M-H]^-$	beta-Carboline	HMDB0012897
170.88371	170.88372	0.05852	CaO_4S	$[M+Cl]^-$	Calcium sulfate	HMDB0303525
172.99143	172.99140	0.17342	$C_6H_6O_4S$	$[M-H]^-$	O-Phenolsulfonic acid	HMDB0304953
172.99143	172.99140	0.17342	$C_6H_6O_4S$	$[M-H]^-$	Phenol sulphate*‡	HMDB0060015
179.05613	179.05611	0.11170	$C_6H_{12}O_6$	$[M-H]^-$	Glucose*†‡	HMDB0304632
185.05681	185.05678	0.16211	$C_7H_{10}N_2O_4$	$[M-H]^-$	2-Amino-2-(5-methyl-3-oxo-1,2-oxazol-4-yl)propanoic Acid	HMDB0257684

185.05681	185.05678	0.16211	$C_7H_{10}N_2O_4$	$[M-H]^-$	alpha-amino-3-hydroxy-5-methyl-4-isoxazolepropionic acid	HMDB0248356
185.05681	185.05678	0.16211	$C_7H_{10}N_2O_4$	$[M-H]^-$	Pyroglutamylglycine	HMDB0061890
185.10845	185.10842	0.16207	$C_{12}H_{14}N_2$	$[M-H]^-$	1-(1-Naphthyl)ethylenediamine*‡	HMDB0255454
185.10845	185.10842	0.16207	$C_{12}H_{14}N_2$	$[M-H]^-$	N-(1-Naphthyl)ethylenediamine	HMDB0254982
186.85610	186.85607	0.16055	FeO_4S	$[M+Cl]^-$	Iron(II) sulfate	HMDB0303497
187.00708	187.00705	0.16042	$C_7H_8O_4S$	$[M-H]^-$	p-Cresol sulfate*	HMDB0011635
191.01975	191.01973	0.10470	$C_6H_8O_7$	$[M-H]^-$	Citric acid*‡	HMDB0000094
194.04588	194.04588	0.00000	$C_9H_9NO_4$	$[M-H]^-$	Salicyluric acid	HMDB0000840
194.04588	194.04588	0.00000	$C_9H_9NO_4$	$[M-H]^-$	3-Hydroxyhippuric acid*	HMDB0006116
195.05105	195.05103	0.10254	$C_6H_{12}O_7$	$[M-H]^-$	Gluconic acid*	HMDB0000625
195.05105	195.05103	0.10254	$C_6H_{12}O_7$	$[M-H]^-$	Galactonic acid	HMDB0000565
195.81092	195.81103	0.56177	Cl_3Fe	$[M+Cl]^-$	Iron(III) chloride	HMDB0303404
198.03275	198.03273	0.10099	$C_9H_{10}ClNO_2$	$[M-H]^-$	N-Chlorophenylalanine*	HMDB0255100
198.03275	198.03273	0.10099	$C_9H_9NO_2$	$[M+Cl]^-$	2-Methyl-2H-1,3-benzoxazin-4(3H)-one	HMDB0249616
198.03275	198.03273	0.10099	$C_9H_{10}ClNO_2$	$[M-H]^-$	(2S)-2-(4-Chloroanilino)propanoic acid	HMDB0243595
198.03275	198.03273	0.10099	$C_9H_9NO_2$	$[M+Cl]^-$	6-Hydroxy-3,4-dihydro-2(1H)-quinolinone	HMDB0246939
198.03275	198.03273	0.10099	$C_9H_{10}ClNO_2$	$[M-H]^-$	4-Chloro-L-phenylalanine	HMDB0244605
213.01718	213.01714	0.18778	$C_6H_{11}ClO_6$	$[M-H]^-$	Glucose chloride	HMDB0252774
213.01718	213.01714	0.18778	$C_6H_{10}O_6$	$[M+Cl]^-$	Gluconolactone	HMDB0000150
215.03283	215.03279	0.18602	$C_6H_{12}O_6$	$[M+Cl]^-$	Glucose*†‡	HMDB0304632
217.02988	217.03016	1.29014	$C_6H_{12}O_6$	$[M+Cl]^-$	Glucose*†‡	HMDB0304632
221.01235	221.01233	0.09049	$C_{10}H_6N_2O_2$	$[M+Cl]^-$	Tyrphostin 23*	HMDB0259354
243.06228	243.06226	0.08228	$C_9H_{12}N_2O_6$	$[M-H]^-$	Uridine*	HMDB0000296
243.06228	243.06226	0.08228	$C_9H_{12}N_2O_6$	$[M-H]^-$	Pseudouridine*	HMDB0000767
257.05464	257.05459	0.19451	$C_7H_{14}N_2O_6$	$[M+Cl]^-$	beta-D-Glucopyranosylurea*†‡	HMDB0249119
257.05464	257.05459	0.19451	$C_7H_{14}N_2O_6$	$[M+Cl]^-$	Glucosamine, N-carbamoyl-(6Cl)	HMDB0248482

263.10374	263.10373	0.03801	$C_{13}H_{16}N_2O_4$	$[M-H]^-$	Phenylacetyl glutaminate	HMDB0256432
263.10374	263.10373	0.03801	$C_{13}H_{16}N_2O_4$	$[M-H]^-$	N(2)-phenylacetyl-L-glutaminate	HMDB0062645
263.10374	263.10373	0.03801	$C_{13}H_{16}N_2O_4$	$[M-H]^-$	di-Hydroxymelatonin*	HMDB0061136
263.10374	263.10373	0.03801	$C_{13}H_{16}N_2O_4$	$[M-H]^-$	Phenylacetylglutamine*	HMDB0006344
263.10374	263.10373	0.03801	$C_{13}H_{16}N_2O_4$	$[M-H]^-$	Acetyl-N-formyl-5-methoxykynurenamine*	HMDB0004259
269.05436	269.05434	0.07433	$C_{12}H_9F_3N_2O_2$	$[M-H]^-$	Leflunomide*†‡	HMDB0015229
274.10451	274.10446	0.18241	$C_{10}H_{17}N_3O_6$	$[M-H]^-$	N-gamma-Glutamylglutamine	HMDB0029147
274.10451	274.10446	0.18241	$C_{10}H_{17}N_3O_6$	$[M-H]^-$	N2-gamma-Glutamylglutamine	HMDB0011738
279.91787	279.91784	0.10717	$C_2HF_6NO_4S_2$	$[M-H]^-$	1,1,1-Trifluoro-N-((trifluoromethyl)sulfonyl)methanesulfonamide	HMDB0247493
295.12409	295.12407	0.06777	$C_{21}H_{16}N_2$	$[M-H]^-$	2,4,5-Triphenylimidazole	HMDB0245477
321.13442	321.13436	0.18684	$C_{17}H_{22}O_6$	$[M-H]^-$	2-Hydroxyphenylacetic acid glucuronide*†‡	HMDB0240440
325.12275	325.12275	0.00000	$C_{15}H_{22}N_2O_4S$	$[M-H]^-$	Hydroxyhexamide	HMDB0060610
325.12275	325.12275	0.00000	$C_{15}H_{22}N_2O_4S$	$[M-H]^-$	N-(N-Acetylmethionyl)dopamine*†	HMDB0244495
339.17325	339.17325	0.00000	$C_{19}H_{28}O_3$	$[M+Cl]^-$	19-Hydroxytestosterone*†	HMDB0006769
339.17325	339.17325	0.00000	$C_{19}H_{28}O_3$	$[M+Cl]^-$	6beta-Hydroxytestosterone*†	HMDB0006259
349.14592	349.14587	0.14321	$C_{23}H_{18}N_4$	$[M-H]^-$	Sibopirdine	HMDB0258286
369.17412	369.17412	0.00000	$C_{19}H_{30}O_5S$	$[M-H]^-$	5a-Dihydrotestosterone sulfate*†‡	HMDB0006278
369.17412	369.17412	0.00000	$C_{19}H_{30}O_5S$	$[M-H]^-$	Epiandrosterone sulfate*	HMDB0062657
377.08563	377.08561	0.05304	$C_{12}H_{22}O_{11}$	$[M+Cl]^-$	Alpha-Lactose	HMDB0000186
377.08563	377.08561	0.05304	$C_{12}H_{22}O_{11}$	$[M+Cl]^-$	beta-Lactose	HMDB0041627
377.08563	377.08561	0.05304	$C_{12}H_{22}O_{11}$	$[M+Cl]^-$	Maltulose	HMDB0029919
383.13801	383.13792	0.23490	$C_{18}H_{24}N_2O_5$	$[M+Cl]^-$	Enalaprilat	HMDB0041886
387.09645	387.09645	0.00000	$C_{16}H_{20}N_2O_7$	$[M+Cl]^-$	Cotinine glucuronide*†	HMDB0001013
480.14038	480.14038	0.00000	$C_{19}H_{23}N_7O_6$	$[M+Cl]^-$	Tetrahydrofolic acid	HMDB0001846

* Metabolites validated by LC-MS/MS, † Differential metabolites in ADs vs HC, ‡ Differential metabolites in SS vs AS vs SLE vs RA vs HC.

Table S8 12 identified differential metabolites of autoimmune diseases versus healthy controls (ADs vs HC) in urine samples.

Compounds	m/z	Adduct	VIP score	p value	Fold change	Regulated
Ribonic acid	165.0405	$[M-H]^-$	1.4296	7.58E-11	2.1822	↑
Urate radical	166.0133	$[M-H]^-$	1.9023	1.29E-20	3.8919	↑
Ascorbic acid	175.0248	$[M-H]^-$	2.1170	1.68E-25	11.3570	↑
2-O-Methylascorbic acid	189.0405	$[M-H]^-$	1.6618	2.74E-09	4.4211	↑
D-Glucuronic acid	193.0354	$[M-H]^-$	1.4223	4.89E-12	2.6535	↑
Uridine	243.0622	$[M-H]^-$	1.5279	1.25E-10	5.3296	↑
Phenylacetylglutamine	263.1038	$[M-H]^-$	1.1046	3.77E-08	2.1653	↑
beta-D-3-Ribofuranosyluric acid	299.0635	$[M-H]^-$	1.5532	7.87E-10	16.9510	↑
N-Acetylneuraminic acid	308.0988	$[M-H]^-$	1.3626	2.07E-09	30.1490	↑
N4-Acetylcytidine	320.0655	$[M+Cl]^-$	1.1119	1.56E-04	6.6094	↑
Androsterone sulfate	369.1741	$[M-H]^-$	1.0906	2.76E-05	0.4207	↓
Androsterone glucuronide	465.2494	$[M-H]^-$	1.3211	7.82E-06	0.1614	↓

Table S9 6 identified differential metabolites of autoimmune diseases versus healthy controls (ADs vs HC) in serum samples.

Compounds	m/z	Adduct	VIP score	p value	Fold change	Regulated
beta-D-Glucopyranosylurea	257.0546	$[M+Cl]^-$	1.6699	2.24E-10	0.4425	↓
Leflunomide	269.0544	$[M-H]^-$	1.5760	3.50E-05	6.3021	↑
N-(N-Acetylmethionyl)dopamine	325.1228	$[M-H]^-$	1.0814	7.81E-03	2.0098	↑
Hydroxytestosterone	339.1733	$[M+Cl]^-$	1.2576	2.35E-03	2.0608	↑
5a-Dihydrotestosterone sulfate	369.1741	$[M-H]^-$	2.1484	9.30E-17	0.3728	↓
Cotinine glucuronide	387.0965	$[M+Cl]^-$	1.4424	8.37E-05	2.4506	↑

Table S10 Metrics of classifiers for individual autoimmune diseases (ADs) versus healthy controls (HC) with urine samples.

	Model	AUC	Accuracy	F1	Precision	Recall
RA vs HC	Random Forest	0.990	0.946	0.946	0.947	0.946
	Neural Network	0.979	0.968	0.968	0.968	0.968
	Logistic Regression	0.977	0.927	0.927	0.932	0.927
	Support Vector Machine	0.963	0.874	0.873	0.878	0.874
	k-Nearest Neighbor	0.945	0.868	0.868	0.873	0.868
	AdaBoost	0.935	0.935	0.935	0.936	0.935
	Naive Bayes	0.898	0.823	0.819	0.848	0.823
SLE vs HC	Random Forest	0.990	0.947	0.947	0.948	0.947
	Naive Bayes	0.983	0.921	0.921	0.921	0.921
	Logistic Regression	0.971	0.877	0.877	0.881	0.877
	Neural Network	0.962	0.939	0.939	0.939	0.939
	Support Vector Machine	0.960	0.886	0.885	0.896	0.886
	k-Nearest Neighbor	0.923	0.842	0.842	0.843	0.842
	AdaBoost	0.851	0.851	0.851	0.851	0.851
AS vs HC	Neural Network	0.998	0.979	0.979	0.980	0.979
	Logistic Regression	0.953	0.875	0.875	0.878	0.875
	Random Forest	0.942	0.875	0.875	0.878	0.875
	Naive Bayes	0.920	0.812	0.812	0.817	0.812
	k-Nearest Neighbor	0.871	0.771	0.770	0.775	0.771
	AdaBoost	0.854	0.854	0.854	0.855	0.854
	Support Vector Machine	0.842	0.812	0.812	0.813	0.812
SS vs HC	Neural Network	0.952	0.952	0.952	0.957	0.952
	Random Forest	0.952	0.881	0.881	0.882	0.881
	Logistic Regression	0.898	0.833	0.831	0.853	0.833
	AdaBoost	0.881	0.881	0.881	0.882	0.881
	Support Vector Machine	0.859	0.714	0.704	0.751	0.714
	Naive Bayes	0.828	0.786	0.783	0.803	0.786
	k-Nearest Neighbor	0.734	0.667	0.664	0.673	0.667

RA: rheumatoid arthritis, SLE: systemic lupus erythematosus, AS: ankylosing spondylitis, SS: sicca syndrome.

Table S11 Metrics of classifiers for individual autoimmune diseases (ADs) versus healthy controls (HC) with serum samples.

	Model	AUC	Accuracy	F1	Precision	Recall
	Neural Network	0.989	0.954	0.954	0.954	0.954
	Support Vector Machine	0.987	0.938	0.938	0.939	0.938
	Logistic Regression	0.967	0.892	0.892	0.893	0.892
RA vs HC	Random Forest	0.962	0.892	0.892	0.893	0.892
	Naive Bayes	0.911	0.817	0.817	0.818	0.817
	k-Nearest Neighbor	0.853	0.758	0.758	0.760	0.758
	AdaBoost	0.833	0.833	0.833	0.833	0.833
	Neural Network	0.998	0.974	0.974	0.974	0.974
	Logistic Regression	0.997	0.965	0.965	0.965	0.965
	Support Vector Machine	0.997	0.965	0.965	0.967	0.965
SLE vs HC	Random Forest	0.991	0.956	0.956	0.956	0.956
	Naive Bayes	0.973	0.912	0.912	0.921	0.912
	k-Nearest Neighbor	0.923	0.842	0.842	0.846	0.842
	AdaBoost	0.921	0.921	0.921	0.924	0.921
	Logistic Regression	0.991	0.958	0.958	0.958	0.958
	Neural Network	0.979	0.938	0.937	0.938	0.938
	Support Vector Machine	0.964	0.875	0.875	0.878	0.875
AS vs HC	Random Forest	0.919	0.812	0.812	0.813	0.812
	AdaBoost	0.917	0.917	0.917	0.920	0.917
	Naive Bayes	0.891	0.792	0.791	0.794	0.792
	k-Nearest Neighbor	0.783	0.750	0.750	0.752	0.75
	Neural Network	0.989	0.905	0.905	0.905	0.905
	Support Vector Machine	0.927	0.857	0.857	0.860	0.857
	Logistic Regression	0.902	0.810	0.809	0.812	0.81
SS vs HC	Naive Bayes	0.891	0.833	0.833	0.834	0.833
	Random Forest	0.866	0.833	0.833	0.834	0.833
	k-Nearest Neighbor	0.807	0.714	0.714	0.714	0.714
	AdaBoost	0.714	0.714	0.714	0.714	0.714

RA: rheumatoid arthritis, SLE: systemic lupus erythematosus, AS: ankylosing spondylitis, SS: sicca syndrome.

Table S12 Metrics of Neural Network for different classification models with urine samples.

Classification	AUC	Accuracy	F1	Precision	Recall
SLE vs RA	0.976	0.947	0.947	0.947	0.947
AS vs RA	0.995	0.938	0.937	0.938	0.938
SS vs RA	0.939	0.881	0.881	0.882	0.881
OT (5) vs RA	0.956	0.885	0.885	0.885	0.885
OT (5) vs RA vs HC	0.971	0.906	0.906	0.906	0.906
SS vs AS vs SLE vs RA	0.953	0.845	0.845	0.845	0.845

SLE: systemic lupus erythematosus, RA: rheumatoid arthritis, AS: ankylosing spondylitis, SS: sicca syndrome, OT: other autoimmune diseases (SLE, AS, SS, SSc: systemic scleroderma, CTD: connective tissue disease).

Table S13 Metrics of Neural Network for different classification models with serum samples.

Classification	AUC	Accuracy	F1	Precision	Recall
SLE vs RA	0.987	0.921	0.921	0.921	0.921
AS vs RA	0.934	0.896	0.896	0.897	0.896
SS vs RA	0.995	0.952	0.952	0.952	0.952
OT (5) vs RA	0.863	0.774	0.773	0.774	0.774
OT (5) vs RA vs HC	0.947	0.832	0.833	0.834	0.832
SS vs AS vs SLE vs RA	0.873	0.679	0.680	0.685	0.679

SLE: systemic lupus erythematosus, RA: rheumatoid arthritis, AS: ankylosing spondylitis, SS: sicca syndrome, OT: other autoimmune diseases (SLE, AS, SS, SSc: systemic scleroderma, CTD: connective tissue disease).

Table S14 Metrics of classifiers for the distinction of four autoimmune diseases (ADs) and healthy controls (HC) with urine samples.

Model	AUC	Accuracy	F1	Precision	Recall
Neural Network	0.984	0.914	0.915	0.918	0.914
Logistic Regression	0.913	0.733	0.729	0.736	0.733
Naive Bayes	0.907	0.705	0.702	0.741	0.705
Support Vector Machine	0.903	0.657	0.671	0.739	0.657
Random Forest	0.884	0.676	0.675	0.680	0.676
k-Nearest Neighbor	0.847	0.438	0.438	0.440	0.438
AdaBoost	0.815	0.705	0.706	0.714	0.705

SS vs AS vs SLE vs RA vs HC, SS: sicca syndrome, AS: ankylosing spondylitis, SLE: systemic lupus erythematosus, RA: rheumatoid arthritis.

Table S15 Metrics of classifiers for the distinction of four autoimmune diseases (ADs) and healthy controls (HC) with serum samples.

Model	AUC	Accuracy	F1	Precision	Recall
Neural Network	0.924	0.714	0.713	0.713	0.714
Support Vector Machine	0.891	0.667	0.666	0.669	0.667
Logistic Regression	0.861	0.629	0.630	0.634	0.629
Random Forest	0.788	0.505	0.488	0.479	0.505
Naive Bayes	0.775	0.419	0.379	0.403	0.419
AdaBoost	0.708	0.533	0.547	0.565	0.533
k-Nearest Neighbor	0.629	0.267	0.274	0.295	0.267

SS vs AS vs SLE vs RA vs HC, SS: sicca syndrome, AS: ankylosing spondylitis, SLE: systemic lupus erythematosus, RA: rheumatoid arthritis.

Table S16 Metrics of classifiers for the distinction of four autoimmune diseases (ADs) and healthy controls (HC) with fusion model.

Model	AUC	Accuracy	F1	Precision	Recall
Neural Network	0.965	0.838	0.836	0.837	0.838
Logistic Regression	0.958	0.829	0.829	0.828	0.829
Support Vector Machine	0.943	0.771	0.776	0.794	0.771
Naive Bayes	0.936	0.752	0.749	0.774	0.752
Random Forest	0.908	0.714	0.713	0.718	0.714
AdaBoost	0.780	0.648	0.643	0.642	0.648
k-Nearest Neighbor	0.765	0.381	0.375	0.437	0.381

SS vs AS vs SLE vs RA vs HC, SS: sicca syndrome, AS: ankylosing spondylitis, SLE: systemic lupus erythematosus, RA: rheumatoid arthritis.

Table S17 19 identified characteristic metabolites in the distinction of four autoimmune diseases (ADs) and healthy controls (HC) with urine samples.

Compounds	m/z	Adduct	f value	p value	Fisher's LSD
Ribonic acid	165.0405	$[M-H]^-$	6.0610	2.16E-03	AS - HC; AS - RA; AS - SLE; SS - HC; SS - RA; SS - SLE
Urate radical	166.0133	$[M-H]^-$	5.3418	4.21E-03	AS - HC; AS - RA; AS - SLE; SS - HC; SS - RA; SS - SLE
Dehydroascorbic acid	173.0092	$[M-H]^-$	4.4279	9.12E-03	AS - HC; SLE - HC; SS - HC; SLE - RA; SS - RA
Ascorbic acid	175.0248	$[M-H]^-$	7.3539	8.90E-04	AS - HC; AS - SLE; RA - HC; SS - HC; SS - RA; SS - SLE
p-Cresol sulfate	187.0071	$[M-H]^-$	3.3924	2.83E-02	HC - AS; RA - AS; SLE - AS
2-O-Methylascorbic acid	189.0405	$[M-H]^-$	3.6419	2.15E-02	SS - AS; SS - HC; SS - RA; SS - SLE
D-Glucuronic acid	193.0354	$[M-H]^-$	6.8060	1.07E-03	AS - HC; AS - RA; AS - SLE; SS - RA; SS - SLE
3-Hydroxyhippuric acid	194.0459	$[M-H]^-$	4.6607	7.34E-03	SS - AS; SS - HC; SS - RA; SS - SLE
Gluconic acid	195.0511	$[M-H]^-$	10.1100	5.36E-05	AS - HC; AS - RA; SS - AS; SS - HC; SS - RA; SS - SLE
Indoxyl sulfate	212.0023	$[M-H]^-$	6.0193	2.16E-03	SS - AS; SLE - HC; SS - HC; SLE - RA; SS - RA
Uridine	243.0622	$[M-H]^-$	5.7487	2.57E-03	AS - RA; SS - AS; SS - HC; SS - RA; SS - SLE
Phenylacetylglutamine	263.1038	$[M-H]^-$	5.0258	6.11E-03	SLE - AS; SS - AS; SLE - HC; SS - HC
beta-D-3-Ribofuranosyluric acid	299.0635	$[M-H]^-$	3.8230	1.75E-02	SS - HC; SS - RA
N-Acetylneuraminic acid	308.0988	$[M-H]^-$	4.1423	1.19E-02	SS - HC; SS - RA; SS - SLE
N4-Acetylcytidine	320.0655	$[M+Cl]^-$	3.5744	2.32E-02	SS - AS; SS - HC; SS - RA; SS - SLE
5-(3',5'-Dihydroxyphenyl)-gamma-valerolactone-O-glucuronide-O-methyl	397.1143	$[M-H]^-$	3.5495	2.38E-02	HC - AS; HC - SS
5-(3',4',5'-trihydroxyphenyl)-gamma-valerolactone-O-methyl-4'-O-glucuronide	413.1088	$[M-H]^-$	3.2335	3.28E-02	HC - AS; HC - RA; HC - SLE
Androsterone glucuronide	465.2494	$[M-H]^-$	4.3718	9.67E-03	HC - AS; HC - RA; HC - SLE; HC - SS
Cortolone-3-glucuronide	541.2654	$[M-H]^-$	3.7811	1.84E-02	AS - RA; AS - SLE; HC - RA; HC - SLE; SS - RA; SS - SLE

Fisher's LSD: Fisher's least significant difference, AS: ankylosing spondylitis, RA: rheumatoid arthritis, SLE: systemic lupus erythematosus, SS: sicca syndrome.

Table S18 9 identified characteristic metabolites in the distinction of four autoimmune diseases (ADs) and healthy controls (HC) with serum samples.

Compounds	m/z	Adduct	f value	p value	Fisher's LSD
Urate radical	166.0133	[M-H]-	3.8793	2.90E-02	SLE - AS; SLE - HC; SLE - RA; SLE - SS
Phenol sulphate	172.9914	[M-H]-	3.4794	4.31E-02	SLE - AS; SLE - HC; SLE - RA; SLE - SS
1-(1-Naphthyl)ethylenediamine	185.1085	[M-H]-	4.9989	9.08E-03	RA - AS; RA - SLE; RA - SS
Citric acid	191.0198	[M-H]-	5.4818	4.88E-03	SLE - AS; SLE - HC; SLE - RA; SLE - SS
Glucose	215.0328	[M+Cl]-	7.8134	3.37E-04	HC - AS; RA - AS; AS - SLE; HC - SLE; HC - SS; RA - SLE; RA - SS
beta-D-Glucopyranosylurea	257.0546	[M+Cl]-	9.2433	7.37E-05	HC - AS; RA - AS; HC - RA; HC - SLE; HC - SS; RA - SLE
Leflunomide	269.0544	[M-H]-	4.5383	1.58E-02	RA - AS; SLE - AS; RA - HC; SLE - HC
2-Hydroxyphenylacetic acid glucuronide	321.1344	[M-H]-	8.1178	2.49E-04	AS - HC; AS - SLE; RA - HC; SS - HC; RA - SLE; SS - SLE
5a-Dihydrotestosterone sulfate	369.1741	[M-H]-	5.4461	4.88E-03	AS - SLE; AS - SS; HC - RA; HC - SLE; HC - SS

Fisher's LSD: Fisher's least significant difference, AS: ankylosing spondylitis, RA: rheumatoid arthritis, SLE: systemic lupus erythematosus, SS: sicca syndrome.

References

1. J. Demsar, G. Leban and B. Zupan, *Journal of Biomedical Informatics*, 2007, **40**, 661-671.
2. H. Zhang, L. Zhao, J. Jiang, J. Zheng, L. Yang, Y. Li, J. Zhou, T. Liu, J. Xu, W. Lou, W. Yang, L. Tan, W. Liu, Y. Yu, M. Ji, Y. Xu, Y. Lu, X. Li, Z. Liu, R. Tian, C. Hu, S. Zhang, Q. Hu, Y. Deng, H. Ying, S. Zhong, X. Zhang, Y. Wang, H. Wang, J. Bai, X. Li and X. Duan, *Nat Commun*, 2022, **13**, 617.